Technology Overview

Evaluating Natural Source Zone Depletion at Sites with LNAPL

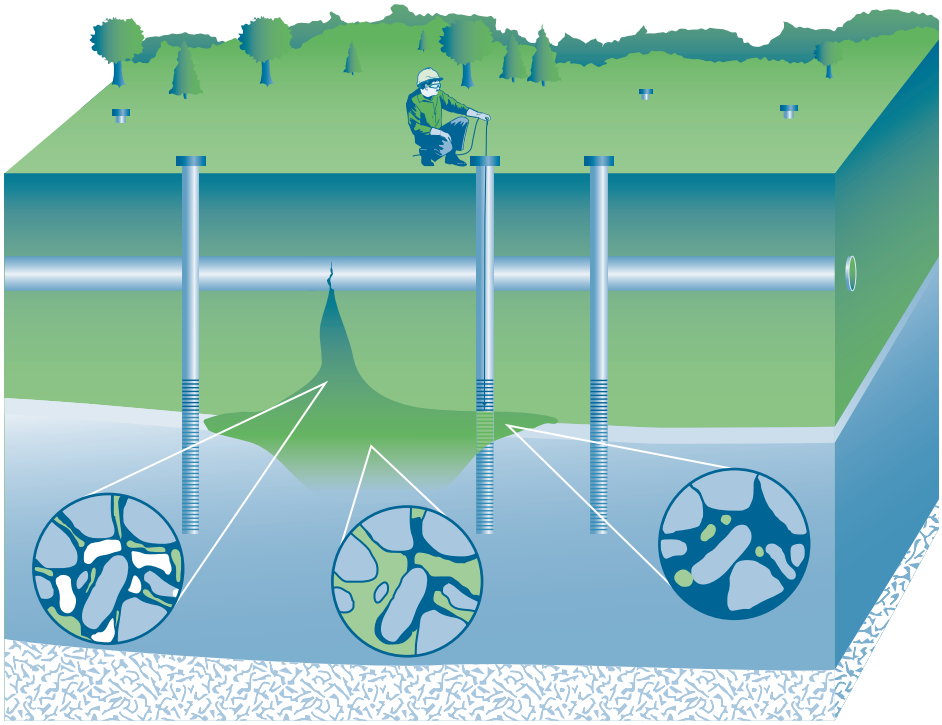

April 2009

Prepared by
The Interstate Technology & Regulatory Council
LNAPLs Team

ABOUT ITRC

Established in 1995, the Interstate Technology & Regulatory Council (ITRC) is a state-led, national coalition of personnel from the environmental regulatory agencies of all 50 states and the District of Columbia, three federal agencies, tribes, and public and industry stakeholders. The organization is devoted to reducing barriers to, and speeding interstate deployment of, better, more cost-effective, innovative environmental techniques. ITRC operates as a committee of the Environmental Research Institute of the States (ERIS), a Section 501(c)(3) public charity that supports the Environmental Council of the States (ECOS) through its educational and research activities aimed at improving the environment in the United States and providing a forum for state environmental policy makers. More information about ITRC and its available products and services can be found on the Internet at www.itrcweb.org.

DISCLAIMER

ITRC documents and training are products designed to help regulators and others develop a consistent approach to their evaluation, regulatory approval, and deployment of specific technologies at specific sites. Although the information in all ITRC products is believed to be reliable and accurate, the product and all material set forth within are provided without warranties of any kind, either express or implied, including but not limited to warranties of the accuracy or completeness of information contained in the product or the suitability of the information contained in the product for any particular purpose. The technical implications of any information or guidance contained in ITRC products may vary widely based on the specific facts involved and should not be used as a substitute for consultation with professional and competent advisors. Although ITRC products attempt to address what the authors believe to be all relevant points, they are not intended to be an exhaustive treatise on the subject. Interested parties should do their own research, and a list of references may be provided as a starting point. ITRC products do not necessarily address all applicable health and safety risks and precautions with respect to particular materials, conditions, or procedures in specific applications of any technology. Consequently, ITRC recommends also consulting applicable standards, laws, regulations, suppliers of materials, and material safety data sheets for information concerning safety and health risks and precautions and compliance with then-applicable laws and regulations. The use of ITRC products and the materials set forth herein is at the user's own risk. ECOS, ERIS, and ITRC shall not be liable for any direct, indirect, incidental, special, consequential, or punitive damages arising out of the use of any information, apparatus, method, or process discussed in ITRC products. ITRC product content may be revised or withdrawn at any time without prior notice.

ECOS, ERIS, and ITRC do not endorse or recommend the use of, nor do they attempt to determine the merits of, any specific technology or technology provider through ITRC training or publication of guidance documents or any other ITRC document. The type of work described in any ITRC training or document should be performed by trained professionals, and federal, state, and municipal laws should be consulted. ECOS, ERIS, and ITRC shall not be liable in the event of any conflict between ITRC training or guidance documents and such laws, regulations, and/or ordinances. Mention of trade names or commercial products does not constitute endorsement or recommendation of use by ECOS, ERIS, or ITRC. The names, trademarks, and logos of ECOS, ERIS, and ITRC appearing in ITRC products may not be used in any advertising or publicity, or otherwise indicate the sponsorship or affiliation of ECOS, ERIS, and ITRC with any product or service, without the express written permission of ECOS, ERIS, and ITRC.

LNAPL-1

Evaluating Natural Source Zone Depletion at Sites with LNAPL

April 2009

Prepared by
The Interstate Technology & Regulatory Council
LNAPLs Team

ACKNOWLEDGEMENTS

The members of the Interstate Technology & Regulatory Council (ITRC) LNAPLs Team wish to acknowledge the individuals, organizations, and agencies that contributed to this technical overview.

Within the broader ITRC effort, the LNAPLs Team effort is funded primarily by members of the Industry Affiliates Program. Additional funding and support have been provided by the U.S. Departments of Energy and Defense and the U.S. Environmental Protection Agency (EPA). ITRC operates as a committee of the Environmental Research Institute of the States (ERIS), a Section 501(c)(3) public charity that supports the Environmental Council of the States (ECOS) through its educational and research activities aimed at improving the environment in the United States and providing a forum for state environmental policy makers.

The work team specifically acknowledges the research efforts of Dr. Paul C. Johnson (Arizona State University), Dr. Paul Lundegard (Lundegard USA), and Dr. Zhuang Liu (Arizona State University), upon whose publications this document is largely founded.

Work team contributing authors:

William "Tripp" Fischer, P.G., Delaware Department of Natural Resources and Environmental Control (LNAPLs Team Co-Leader)
Charles D. Stone, P.G., P.E., Texas Commission on Environmental Quality (NSZD Subteam Leader)
Harley Hopkins, American Petroleum Institute
Mark Lyverse, Chevron Energy Technology Co.
John Menatti, P.G., Utah Department of Environmental Quality
Eric M. Nichols, P.E., LFR (ARCADIS)
Joel P. Padgett, South Carolina Department of Health and Environmental Control
Tim J. Smith, Chevron Energy Technology Co.
John D. Surber, Jr., Virginia Department of Environmental Quality
Lesley Hay Wilson, Ph.D., Sage Risk Solutions LLC

Valuable comments on document drafts were provided by:

Pam Trowbridge, P.G., Pennsylvania Department of Environmental Protection (LNAPLs Team Co-Leader)
Chet Clarke, P.G., AMEC Geomatrix, Inc.
Paul C. Johnson, Ph.D., Arizona State University
Terrence Johnson, Ph.D., EPA Environmental Response Team
Paul Lundegard, R.G., Ph.D., Lundegard USA
Issis Rivadineyra, Naval Facilities Engineering Center
Michael Singletary, Naval Facilities Engineering Center
Ronald Wallace, Georgia Department of Natural Resources

EXECUTIVE SUMMARY

Light, nonaqueous-phase liquid (LNAPL) refers to an organic compound that is immiscible with, and lighter than, water (e.g., crude oil, gasoline, diesel fuel, heating oil). When an LNAPL is released to the subsurface, it can migrate downward under the force of gravity and laterally at the water table. Larger LNAPL releases may migrate to the water table while leaving residual, immobile LNAPL along the migration path.

The constituents, or chemicals, that compose the LNAPL may be removed over time by various mechanisms, such as sorption, volatilization, and dissolution. If not removed, the LNAPL "body" can function as a potentially long-lived source zone for secondary impacts to adjacent soil, soil gas, and groundwater.

A simple, quantitative mass balance assessment of source zones could conclude that, if some quantities of constituents are **naturally** being lost from the source zone at some rate due to natural processes, then the source zone itself must be depleting to some degree. The key question then becomes, at what rate is this natural source zone depletion (NSZD) occurring? This document addresses this and other questions associated with NSZD, including the following:

- What are the NSZD processes?
- What are the NSZD rates?
- What will the NSZD look like in the future?

NSZD is of significance because it occupies a position in the spectrum of remediation options that can be used as a basis for comparing the performance and relative benefit of other remediation options. It is also of significance because engineered remedial actions typically do not always completely remediate soils and NSZD may be useful to address the residual hydrocarbon.

Although the challenging issue is deciding the applicability of NSZD, this document addresses only the technical process for evaluating NSZD in the context of the questions listed above. It does not discuss applicability of NSZD in the remedial decision-making process. Regulatory matters, such as the applicability of NSZD in a remedial decision-making process, will be addressed in a forthcoming LNAPLs Team technical/regulatory guidance document to be entitled *Evaluating LNAPL Remedial Technologies for Achieving Project Goals.* This technical overview document is a companion to that guidance document.

The LNAPLs Team comprises representatives of state and federal regulatory agencies, the U.S. Department of Defense, public stakeholders, oil companies, the American Petroleum Institute, environmental consultants, and vendors. This technical overview document was developed by a subgroup of the LNAPLs Team that reflects the general composition of the team as a whole.

TABLE OF CONTENTS

LIST OF TABLES

LIST OF FIGURES

APPENDICES

EVALUATING NATURAL SOURCE ZONE DEPLETION AT SITES WITH LNAPL

1. INTRODUCTION

Numerous sites across the country are impacted with light, nonaqueous-phase liquids (LNAPLs). LNAPL recovery is often a default or presumptive remedial objective in most regulatory programs. Unfortunately, LNAPLs have historically posed a significant challenge to site remediation for various reasons. A variety of passive and active remedial technologies exist that have applicability to different LNAPL and site conditions. This document provides a technical overview of natural source zone depletion (NSZD) for LNAPLs, which, when appropriately evaluated, can serve as an objective benchmark by which to compare the relative effectiveness of different remedial alternatives.

1.1 LNAPL Source Zones

"LNAPL" is a term given to an organic compound that is immiscible with, and lighter than, water (e.g., crude oil, gasoline, diesel fuel, heating oil). When an LNAPL is released to the subsurface, it can migrate downward and laterally. The resulting LNAPL distribution depends on soil properties (such as grain size and porosity), nonaqueous-phase liquid (NAPL) properties (such as viscosity), and the LNAPL release volume.

Small LNAPL releases may become trapped in the soil pores as an immobile, residual phase before it is able to reach to the water table. Larger LNAPL releases may migrate to the water table while leaving immobile, residual LNAPL along the migration path. At the water table, LNAPL can accumulate and actually spread across the surface of the saturated zone, predominantly in the direction of decreasing hydraulic gradient. The constituents, or chemicals, that compose the LNAPL may be removed over time by various mechanisms, such as sorption, volatilization, and dissolution. If not removed, the LNAPL "body" can function as a potentially long-lived source of secondary impacts to adjacent soil, soil gas, and groundwater. This document refers to such an LNAPL body as a "source zone." Figure 1-1 shows an example LNAPL source zone in cross section. The portion of the source zone in the unsaturated zone is referred to as the unsaturated, or exposed, source zone. The portion of the source zone in the groundwater-saturated zone or below the water table is referred to as the saturated, or submerged, source zone.

1.2 Natural Source Zone Depletion

A simple, quantitative mass balance assessment of source zones could conclude that, if some quantities of chemicals are being *naturally* lost from the source zone at some rate due to volatilization, dissolution, biodegradation, and sorption, then the source zone itself must be depleting to some degree. This document addresses several questions associated with NSZD:

- What are the NSZD rates?
- What are the NSZD processes?
- What will the NSZD look like in the future?

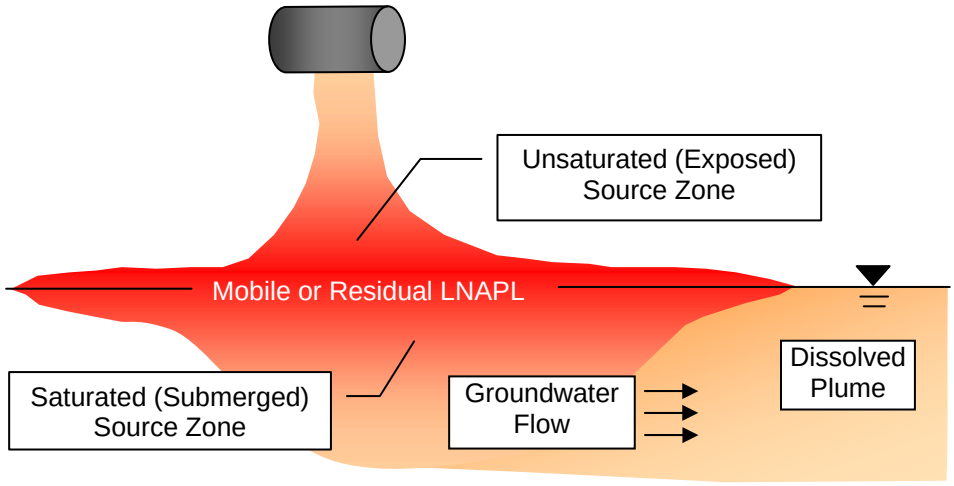

Figure 1-1. Example LNAPL source zone.

Understanding the answers to these questions benefits the remedial decision-making process for any site impacted with LNAPL; however, this document does not discuss applicability of NSZD in that process. Risk assessment and resource protection are also not addressed. This document is meant only to answer the questions above.

NSZD is of significance because it occupies a position in the spectrum of remediation options which can be used as a basis for comparing the performance and relative benefit of other remediation options. It is also of significance because engineered remedial actions typically do not completely remove all LNAPL from soils and NSZD may be useful to address the residual hydrocarbon. This document assumes that an overall corrective action program is being implemented during this NSZD evaluation process.

2. LNAPL NSZD PROCESSES

LNAPL NSZD occurs when certain processes act to (a) physically redistribute LNAPL components to the aqueous or gaseous phase and (b) biologically break down source zone components. This section describes the various processes responsible for NSZD.

NSZD is a combination of processes that reduce the mass of LNAPL in the subsurface. These processes include dissolution of LNAPL constituents into groundwater and volatilization of LNAPL constituents into the vadose zone. In turn, LNAPL constituents dissolved to groundwater and volatilized to the vadose zone can be biodegraded by microbial and/or enzymatic activity. Biodegradation rates depend on the type and availability of electron acceptors (oxygen, nitrate, sulfate, ferrous iron, manganese, and methane) in the subsurface soils and groundwater.

2.1 LNAPL Dissolution into Groundwater and Biodegradation in the Saturated Zone

Portions of source zones that are submerged below the water table are subject to dissolution of LNAPL constituents into groundwater according to the constituents' aqueous solubility. Source zone mass is lost as the dissolved-phase constituents leave the source zone via groundwater

transport. Figure 2-1 depicts the basic elements of the source zone dissolution and biodegradation mass depletion processes in groundwater.

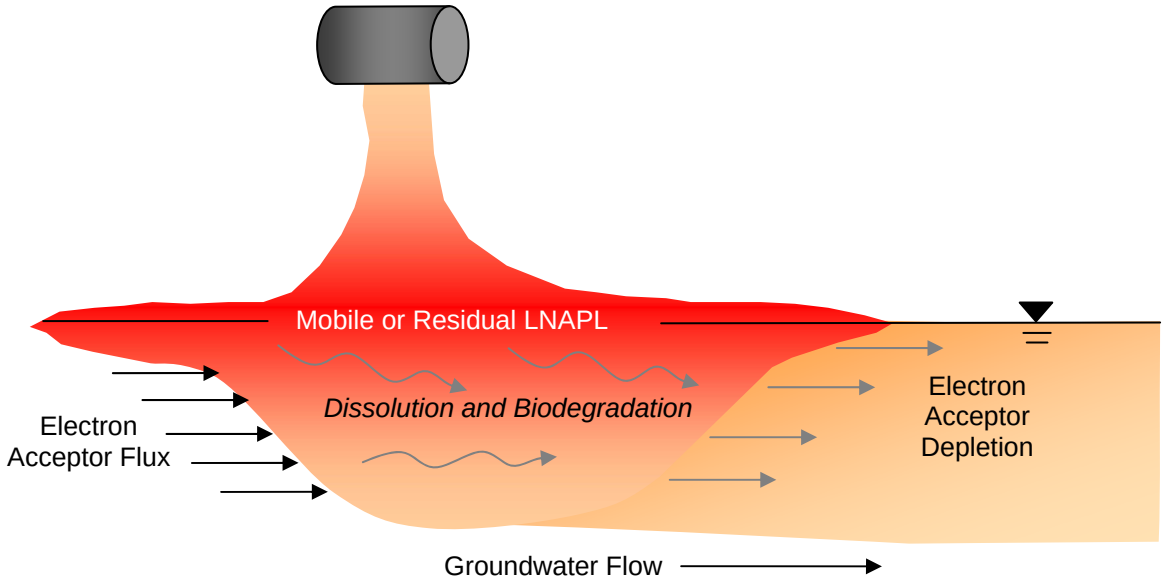

Figure 2-1. Groundwater transport–related NSZD processes.

NSZD by groundwater dissolution and biodegradation processes is controlled primarily by the following:

- solubility and effective solubility
- availability of electron acceptors
- groundwater flow under, around, and through the LNAPL source

While LNAPL recovery from the source zone can result in reducing the LNAPL to residual saturation, LNAPL dissolution continues in the saturated zone according to its solubility.

"Effective solubility" represents the maximum equilibrium concentration of a constituent from a multicomponent LNAPL mixture in groundwater at a specific temperature and pressure (EPA 1995). Effective solubility (S^e_i) of an individual LNAPL constituent is a product of its mole fraction in the LNAPL (X_i) and solubility of the constituents in its pure phase (S_i):

$$S_i^e = X_i S_i \qquad \textbf{[Eq. 2-1]}$$

Zemo (2006) reports average theoretical effective solubilities of gasoline and diesel, as well as averages from several studies by other authors. Other studies reporting effective solubility estimates for gasoline include EPA (1996); Morrison, Beers, and Hartman (1998); and Falta and Bulsara (2004). However, in many cases, it may be necessary to determine a site-specific effective solubility value of actual on-site LNAPL using standard test methods (e.g., ASTM Standard E1148) and Equation 2-1.

As LNAPL weathers, the effective solubility (Equation 2-1) of its constituents decreases. The data provided by the EPA (1996) exhibit the differences in degree of weathering between different gasoline samples. Decreases of effective solubility over time, as evidenced by decreasing dissolved-phase concentrations in the source zone, give further evidence of NSZD.

Increases in dissolved-phase petroleum hydrocarbon concentrations between upgradient and downgradient monitor wells are evidence that dissolution is occurring (Johnson, Lundegard, and Liu 2006). Biodegradation of dissolved petroleum hydrocarbon plumes in groundwater has been well documented. Biodegradation of dissolved-phase petroleum hydrocarbon plumes is reflected in spatial changes in concentrations of dissolved electron acceptors (oxygen, nitrate, and sulfate) and dissolved biodegradation products (reduced manganese, ferrous iron, hydrogen, organic acids, and methane).

Natural biodegradation processes act to reduce dissolved-phase plume mass originating from the source zone. Benzene plume lengths tend to stabilize at relatively short distances from the source zone (e.g., BEG 1997). While microorganisms metabolize petroleum hydrocarbons as a carbon and energy source, the specific mechanisms by which petroleum hydrocarbons are degraded are not completely understood. However, empirical knowledge of this phenomenon can be incorporated into the management of site investigations and remediation.

Groundwater scientists recognize that the major factor responsible for shorter, stable dissolved hydrocarbon plumes is aerobic and anaerobic microbial metabolism (Scow 1982; Barker, Patrick, and Major 1987; Rifai et al. 1988; Chiang et al. 1989; Cozzarelli, Eganhouse, and Baedecker 1990; Cozzarelli et al. 1994; Baedecker et al. 1992, 1993; Bennett et al. 1993; Daniel 1993; Eganhouse et al. 1993; Salanitro 1993; NRC 1994; Borden, Gomez, and Becker 1995; McNab and Narasimhan 1995).

As groundwater flows about the submerged source zone, petroleum hydrocarbon constituents dissolve into the groundwater and are transported downgradient. Naturally occurring microbial populations in the saturated zone degrade petroleum hydrocarbon constituents to organic acid intermediates and finally to carbon dioxide and water. The microbes preferentially use oxygen as an electron acceptor. As oxygen is depleted, other electron acceptors are used, such as nitrate, sulfate, ferric iron, and manganese (Cozzarelli and Baedecker 1992, Salanitro et al. 1993). This process results in an area of the dissolved-phase plume core in which oxygen, nitrate, sulfate, ferric iron, pH, and oxidation-reduction potential measurements are depleted and ferrous (reduced) iron is enriched relative to the background groundwater geochemistry.

The biodegradation of hydrocarbons proceeds most rapidly under aerobic conditions. The ability of microorganisms to degrade petroleum hydrocarbons may be limited by the availability of electron acceptors (Bouwer and McCarty 1984; Vogel, Criddle, and McCarty 1987). Naturally occurring groundwater geochemistry often controls the electron acceptor supply. In other situations, the availability of electron acceptors may not be limiting, resulting in an excess capacity for microbial petroleum hydrocarbon biodegradation (Wilson et al. 1994). The quantitative analysis of biodegradation is discussed in Section 3.5.

2.2 LNAPL Volatilization and Biodegradation in the Vadose Zone

Some mass in LNAPL source zones within the vadose zone is subject to redistribution as soil gas due to volatilization of hydrocarbon constituents. Hydrocarbon vapors then migrate through the vadose zone soils by diffusive and advective processes. Figure 2-2 depicts the basic components of source zone volatilization and biodegradation depletion processes in the vadose zone.

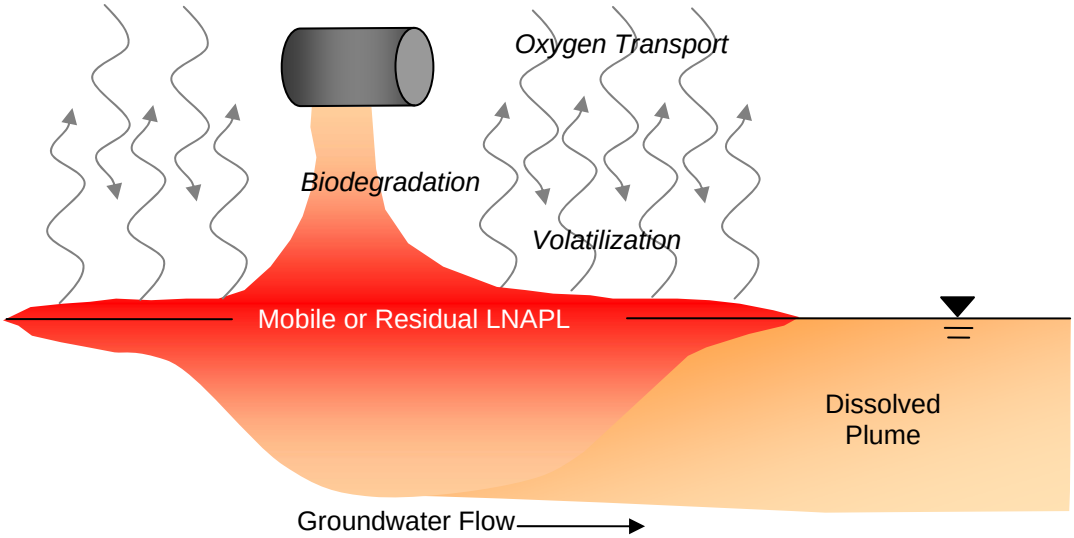

Figure 2-2. Vapor transport–related NSZD processes.

Volatile constituents move from areas of higher concentration to areas of lower concentration. In the subsurface, constituent vapors preferentially migrate from subsurface contaminant source areas towards the ground surface. Diffusion is usually the dominant mechanism for vapor-phase transport in unsaturated porous media under most natural conditions (Rockhold, Yarwood, and Selker 2004) and is a function of a constituent's air diffusion coefficient and the air-filled porosity of the soil. Diffusion and vapor migration are faster in soils with more air-filled effective porosity, such as sand with low moisture content.

Advection is the movement of bulk soil gas and is driven by pressure gradients. Bulk soil gas moves from areas of higher pressure to areas of lower pressure. Vapor extraction wells can induce advective movement of bulk soil gas in vadose zone soils. Natural and artificial barometric pressure gradients can result in underpressurized buildings, thereby inducing advective flow of bulk soil gas and resulting in vapor intrusion through cracked building slabs, floors, and utilities (see ITRC 2007a, b). Relatively thin soil layers with different soil properties (e.g., a layer of silty soil in medium-grained sand) can have a significant effect on the transport of vapors through unsaturated soils (DeVaull, Ettinger, and Gustafson 2002).

Biodegradation of petroleum hydrocarbon vapors is well documented:

- EPA (1987) described the biodegradation of gasoline and other petroleum vapors by the genera *Pseudomonas* and *Arthrobacter*, which are heterotrophic bacteria commonly present in soil (Alexander 1977).

- Microbes capable of aerobic biodegradation of petroleum constituents are present in almost every soil (e.g., DeVaull, Ettinger, and Gustafson 2002).

- Ostendorf and Kampbell (1991) concluded that biodegradation of petroleum hydrocarbon vapor at a U.S. Coast Guard Station in Traverse City, Michigan prevents the escape of appreciable hydrocarbon-vapor contamination to the atmosphere.

- DeVaull et al. (1997) reported that oxygen concentrations above 4% in the vadose zone are adequate for substantial biodegradation of benzene, toluene, ethylbenzene, and xylenes (BTEX) constituents to occur in a short distance.

- At a petroleum release site in Stafford, New Jersey, soil gas sampling at various depths over a shallow dissolved-phase gasoline plume indicated that biodegradation was responsible for attenuating benzene vapor concentrations upward through a sandy vadose zone soil (Sanders and Hers 2006).

- Ririe and Sweeny (1996) and Ririe, Sweeny, and Daugherty (2002) report from field sampling studies conducted at three California sites that the diffusive transport of benzene can be effectively retarded (adsorption and biodegradation) by an overburden soil column of 2–3 feet of uncontaminated soil. These studies concluded that biodegradation is primarily responsible for the observed attenuation of benzene vapors in the vadose zone and that models that do not account for biodegradation may overestimate benzene vapor risks by a factor of 500–1000. However, be aware of site conditions that may enhance vapor migration, such as subsurface fractures and underground utilities that may provide preferential flow paths for vapors from the subsurface to migrate into buildings.

- Field evidence indicates that biodegradation is a key factor that may greatly reduce the spreading distance, the maximum gaseous concentrations, and the time to depletion for all biodegradable mixture components, especially for those with a high aqueous solubility and a low Henry's constant (e.g., benzene) (Gaganis, Kjeldsen, and Burganos 2004).

2.3 Direct Biodegradation of LNAPL

Biodegradation of LNAPL source zones via microbial activity in the aqueous phase and vapor phase has been described and documented. However, there is less literature on the subject of direct biodegradation of the nonaqueous phase in the subsurface, examples of which include the demonstration of biodegradation of residual NAPL by Stout and Lundegard (1998). Although it is commonly assumed that biodegradation or mineralization of source zone constituent mass is limited by the rate of partitioning from the LNAPL to aqueous phase, several laboratory studies have shown that rates of mineralization of target constituents dissolved into solvents (NAPLs) have exceeded the measured rates of partitioning. These studies propose various mechanisms for bacteria to enhance biodegradation of the LNAPL constituents and are discussed in more detail in Appendix D.

Birman and Alexander (1996) studied the effect of NAPL viscosity on biodegradation of phenanthrene in several different NAPLs in soil slurries. Efroymson and Alexander (1991,

1994b); Ortega-Calvo and Alexander (1994); and Ortega-Calvo, Birman, and Alexander (1995) found that rates of biodegradation in some cases exceeded the rates of partitioning from NAPL to aqueous phase for reasons discussed in Appendix D. Inoue and Horikoshi (1991) and Efroymson and Alexander (1994a) describe toxicity effects of organic solvents with low oil/water partition coefficients. A study by Kanaly et al. (2000) found that a certain microbial growth on diesel fuel likely caused emulsification of the benzo[a]pyrene in diesel fuel.

Direct biodegradation of LNAPL in the subsurface, where occurring, is likely a slow process. Toxicity of certain LNAPLs to indigenous microbes may serve to minimize or eliminate direct intrinsic biodegradation as a source mass loss mechanism at some sites. Additional studies of degradation of residual NAPL include Douglas et al. (1992) and Prince et al. (1994). Degradation of long-chain LNAPL constituents (e.g., *n*-alkanes) has been demonstrated to occur via extra-cellular enzymatic activity (Bekins et al. 2005, Hostettler et al. 2007), as well as by anaerobes (e.g., Wilkes et al. 1995).

3. NATURAL SOURCE ZONE DEPLETION ASSESSMENT

Assessment and characterization of LNAPL occurrences must include both the vadose zone and the saturated zone when consideration of NSZD is anticipated.

3.1 LNAPL Conceptual Site Model

A complete assessment of the LNAPL body, dissolved-phase plume, vapor plume, potential exposure pathways, and receptors is required before embarking on an NSZD evaluation. This assessment should include complete delineation of the LNAPL body (horizontal extent and vertical extent, including the smear zone), dissolved-phase plume in groundwater, and vapor plume in the vadose zone. Using the data from the assessment, an LNAPL conceptual site model should be developed and presented in plan view maps and cross sections (e.g., see ITRC 2007c). Evaluations of exposure pathways and receptors are necessary to determine acceptable risk when using NSZD.

3.1.1 Site Geology

The site-specific geology associated with an LNAPL release site should be thoroughly evaluated, at a minimum, to identify the potential LNAPL subsurface migration pathways. Locations of areas with variations of soil type, grain size, fracturing, stratigraphy, and other features that can limit or enhance LNAPL migration should be described in detail. Once LNAPL is disseminated in the subsurface, vadose zone NSZD volatilization and biodegradation processes can occur at significant rates. Once the vadose zone geology of the release site is fully characterized and understood, meaningful vadose zone NSZD assessments and NSZD measurements can be performed in support of NSZD demonstrations.

Example Problem: Background and LNAPL Conceptual Site Model

A former service station had a long-term gasoline leak from underground storage tanks. The gasoline migrated through the vadose zone to the groundwater table at about 20 feet below ground surface (bgs). Upon reaching the water table, the LNAPL migrated laterally through sandy sediments towards the southeast about 100 feet, where it stabilized. The LNAPL served as the source zone for a dissolved groundwater hydrocarbon plume which has migrated off site downgradient of the source zone (see map and cross-section).

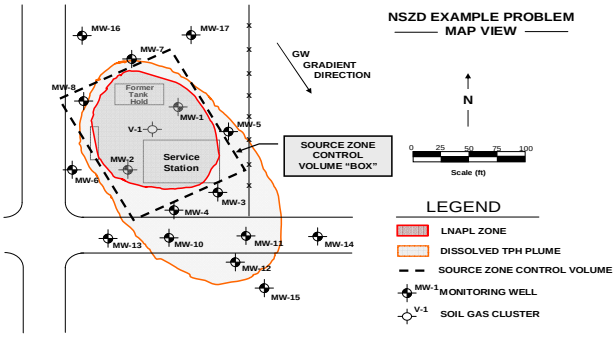

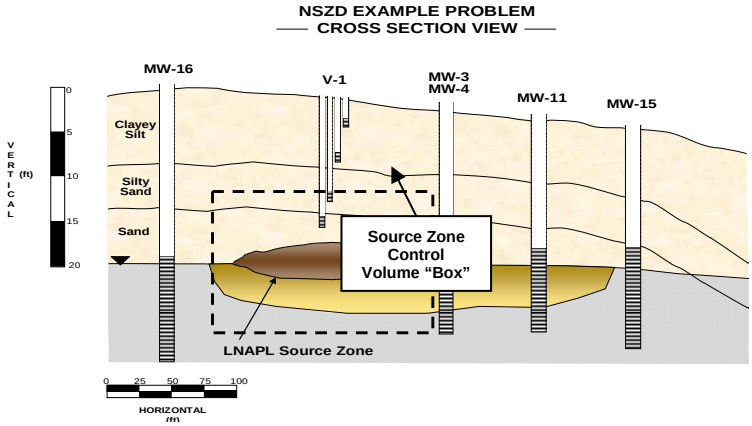

Initial LNAPL remediation efforts recovered approximately 20,000 gal of LNAPL using skimming pumps. When hydraulic free-product removal rates decreased, a multiphase extraction (MPE) pilot test indicated that MPE would not be cost-effective at the site due to low gasoline/water recovery rates and the high cost of water treatment and disposal.

3.1.2 Site Hydrostratigraphy

The site-specific occurrence of groundwater at a release site should be fully investigated and documented when LNAPL is known to have impacted, or is threatening to impact, groundwater. Once LNAPL reaches the capillary fringe of the saturated zone, LNAPL dissolution to groundwater can occur at significant mass depletion rates (e.g., Klenk and Grathwohl 2002). A complete, detailed understanding of the site groundwater system, its behavior, and the distribution of LNAPL therein is essential for the assessment and accounting of saturated zone NSZD processes and accurate NSZD dissolution mass balance determinations.

3.2 Site Dissolved Groundwater Contaminant Concentrations

The distribution and magnitude of dissolved-phase groundwater constituents associated with an LNAPL release at a site can provide vital information about NSZD processes and rates occurring at and within the saturated zone (e.g., Bockelmann, Ptak, and Teutsch 2001). The distribution of dissolved-phase constituents in a groundwater system that is associated with an LNAPL release can provide much information about LNAPL dissolution rates, LNAPL soluble fractions (Section 4.1), background constituent concentrations and mass balance (Section 3.5.2), and potential risk to receptors (Section 4.3). Predictive modeling of NSZD processes for the purpose of estimating remedial time frames and establishing future site "snapshots" depends on obtaining meaningful three-dimensional dissolved-phase plume data and aqueous geochemical indicators. These data are typically required as input parameters for the numerical model packages that are used to create the predictive modeling results (see Section 4.5).

3.3 Site Source Zone Delineation

The nature and distribution of the LNAPL source zone must be fully characterized prior to evaluating NSZD processes. Gaps in the information about the LNAPL distribution can reduce the confidence of NSZD mass depletion calculations and predictions.

3.3.1 Source Zone Mass Estimates

Estimates of LNAPL mass composing the LNAPL source zone must be made to understand the physical scale of the source zone and, ultimately, to facilitate determinations of its longevity when subjected to NSZD processes. Farr, Houghtalen, and McWhorter (1990); Lenhard and Parker (1990); Huntley, Hawk, and Corley (1994); and Lundegard and Johnson (2006) discuss methods by which source zone mass can be estimated.

3.3.2 LNAPL Distribution in the Vadose Zone

The exposed portion of the LNAPL source zone within the vadose zone must be assessed and delineated accordingly. The exposed portion must be distinguished from the submerged source zone (see Section 3.3.3) because it is subject to only the vadose zone mass depletion processes (see Section 2.2). Mass depletion rate calculations based on LNAPL source zone volatilization processes apply to *only* the exposed source zone and are developed separately from the submerged source zone calculations.

3.3.3 LNAPL Distribution in the Saturated Zone

The submerged portion of the LNAPL source zone occurs at and below the capillary fringe within the saturated zone. This portion of the LNAPL zone must be delineated and distinguished from the exposed vadose zone portion of the LNAPL source zone. Mass depletion rate calculations based on LNAPL source zone dissolution processes apply to only submerged portions of the source zone (see Section 2.1). Therefore, it is important to understand its distribution. Since groundwater level fluctuations change the extent of the exposed/submerged source zones, historical water level data should be reviewed and considered when assessing long-term mass loss rates.

3.4 Qualitative NSZD Assessment

Qualitative assessments for NSZD comprise (a) the accumulation of evidence for the occurrence of mass redistribution from the source zone to groundwater and the vadose zone and (b) the identification of which NSZD processes are occurring. At large release sites, which are typically more complex, much of the data needed for the qualitative assessment may be available. At newer or smaller sites, additional data collection may be needed. Figure 3-1 summarizes the basic NSZD qualitative assessment endeavors. Gathering evidence of these processes will highlight data gaps and set the stage for further study of the current and expected mass loss rates. Table 3-1 provides a summary of qualitative NSZD assessment supporting data observations.

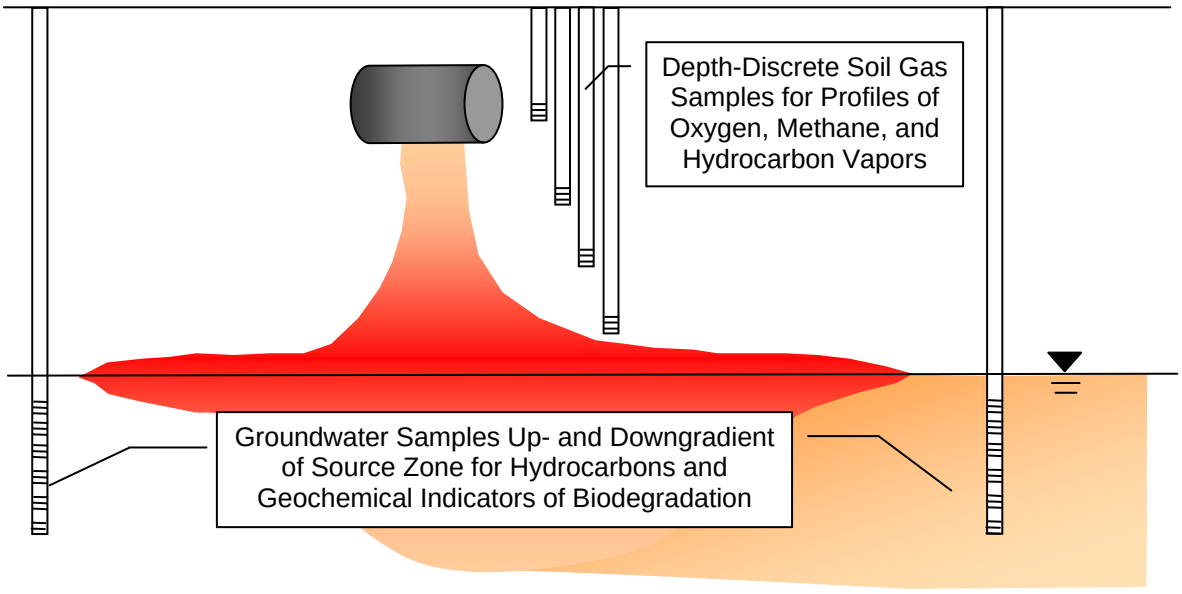

Figure 3-1. Data for qualitative assessment of NSZD.

3.5 Quantitative NSZD Assessment

Quantitative NSZD assessments comprise the collection and evaluation of site data that can be used to determine mass flux rates from LNAPL source zones for each NSZD process.

3.5.1 Introduction

The rate that NSZD is occurring can be estimated by the measurement of dissolution and biodegradation processes in the saturated zone and of volatilization and biodegradation processes in the unsaturated zone. The measurement of each process requires collection of key site-specific data. For dissolution and biodegradation in the saturated zone, the required data include hydraulic parameters; horizontal and vertical dimensions of the LNAPL source zone; and dissolved hydrocarbon, oxygen, nitrate, sulfate, iron, and manganese concentrations upgradient and downgradient of the source zone. Site-specific hydraulic parameters and groundwater chemical data are commonly obtained from monitoring wells. For volatilization and biodegradation in the unsaturated zone, the data required are vertical hydrocarbon soil gas concentration profiles and

vertical oxygen and methane soil gas profiles. Soil gas measurements may be obtained from multilevel soil probes or from conventional borings via the use of inflatable packers.

Table 3-1. Data for qualitative evaluation: Evidence that NSZD is occurring

NSZD process	Supporting data	Purpose
Source zone dissolution to groundwater	Static water elevations at groundwater monitoring wells	Determine the hydraulic gradient and groundwater flow direction (needed to properly interpret dissolved concentration data)
	Dissolved hydrocarbon concentrations in groundwater up- and downgradient of source zone	Increases in dissolved-phase hydrocarbon concentrations between up- and downgradient wells are evidence that dissolution is occurring
Biodegradation of dissolved source zone mass	Dissolved electron acceptor reactant (e.g., O_2, NO_3^-, SO_4^{2-}) and product (e.g., Fe^{2+}, Mn^{2+}) concentrations in groundwater up- and downgradient of the source zone	Decreases in dissolved O_2, NO_3^-, and SO_4^{2-} and increases in Fe^{2+} and Mn^{2+} between up- and downgradient wells are evidence that biodegradation is occurring
	Dissolved methane (CH_4) concentrations in groundwater up- and downgradient of the source zone	Increases in dissolved CH_4 between up- and downgradient wells are evidence that anaerobic biodegradation is occurring via methanogenesis
Source zone volatilization to vadose zone	Hydrocarbon soil-gas concentration profiles	Decreasing hydrocarbon concentrations in soil gas with distance from the source zone are evidence that volatilization of source zone is occurring
	Total petroleum hydrocarbon (TPH) composition in soil, unweathered (‘‘fresh’’) LNAPL-containing soils (or free product)	Changes in the hydrocarbon composition in soil relative to the initial hydrocarbon composition could also be evidence of NSZD and could reflect the combined effect of mass loss mechanisms
Biodegradation of volatilized source zone mass	Respiration and biogenic soil-gas concentration profiles (O_2, CO_2, CH_4)	Soil-gas profiles with decreasing O_2, increasing CO_2, or increasing CH_4 concentrations with depth to the source zone are consistent with the occurrence of biodegradation (CH_4 can also be produced by natural sources and may be distinguished by carbon stable isotope fractionation or background soil-gas profiles collected away from source zones)
	Soil TPH concentrations with time	May not be practicable—long-term monitoring and large numbers of samples may be necessary to observe trends

Source: Adapted from Johnson, Lundegard, and Liu 2006.

3.5.2 Estimate of Source Zone Mass Depletion Rate by Dissolution to Groundwater

LNAPL dissolution occurs when the source zone is in contact with groundwater (and sometimes with surface recharge water). Dissolved LNAPL components in groundwater are transported from the source zone by groundwater flow. The rate at which this source zone mass is lost can be quantified using a rectilinear control volume “box” that encompasses the margins of the LNAPL source zone volume, as depicted in Figure 3-2. From such a reference diagram, an accounting of NSZD process mass transfers and mass balance can be organized.

Example Problem: Qualitative NSZD Assessment

Numerous groundwater monitoring wells and vadose zone vapor probes were installed in and around the LNAPL source zone (see map and cross section). Groundwater and vapor data from the wells and probes indicated that the LNAPL source zone was continuing to dissolve to the groundwater and to volatilize to the vadose zone. Groundwater geochemistry data indicated that electron acceptor and biodegradation transformation product concentrations upgradient of the source zone were different than corresponding downgradient concentrations (Table A), significantly enough to indicate the occurrence of biodegradation of dissolved hydrocarbon mass.

TABLE A
Dissolved Groundwater Concentrations

			Electron Acceptors (Median)			Biodegradation Transformation Products		
	Well Number	TPH-GRO (C_{10})	Oxygen (mg/L O_2)	Nitrate (mg/L NO_3^-)	Sulfate (mg/L SO_4^{2-})	Iron (mg/L Fe^{2+})	Manganese (mg/L Mn^{2+})	Methane (mg/L CH_4)
Downgradient Wells	MW-3	3.000 mg/L	0.5 mg/L	0.0 mg/L	10.0 mg/L	16.0 mg/L	1.0 mg/L	4.5 mg/L
	MW-4	4.000 mg/L						
Upgradient Wells (Median)	MW-16	ND	5.0 mg/L	4.2 mg/L	40.0 mg/L	0.00 mg/L	0.0 mg/L	0.000 mg/L
	MW-17	ND						

Additionally, soil vapor probe data (time-averaged over two years) located directly over the source zone (Vapor Probe V-1) indicated that, with depth, methane concentrations increased and oxygen concentrations decreased (Table B). [Note: concentrations at depth = 0 ft reflect atmospheric composition values.] These data demonstrated that mass volatilizing from the exposed portion of the NAPL source zone was being biodegraded in the vadose zone.

TABLE B
Soil Vapor Concentrations

Soil Probe (V-1) Depth		Time-Average O_2 Soil Vapor Concentration			Time-Average CH_4 Soil Vapor Concentration		
(ft)	(m)	(%)	(ppm)	(kg O_2/m^3)	(%)	(ppm)	(kg CH_4/m^3)
0.0 ft	0.0 m	20.9%	209470	0.274	0.00017%	1.70	1.11E-06
3.0 ft	0.9 m	15.3%	153300	0.201	0.00027%	2.67	1.75E-06
7.0 ft	2.1 m	16.7%	166700	0.218	0.00030%	3.00	1.96E-06
11.0 ft	3.4 m	12.0%	120000	0.157	0.00025%	2.50	1.64E-06
15.0 ft	4.6 m	4.2%	42300	0.055	0.00443%	44.30	2.90E-05

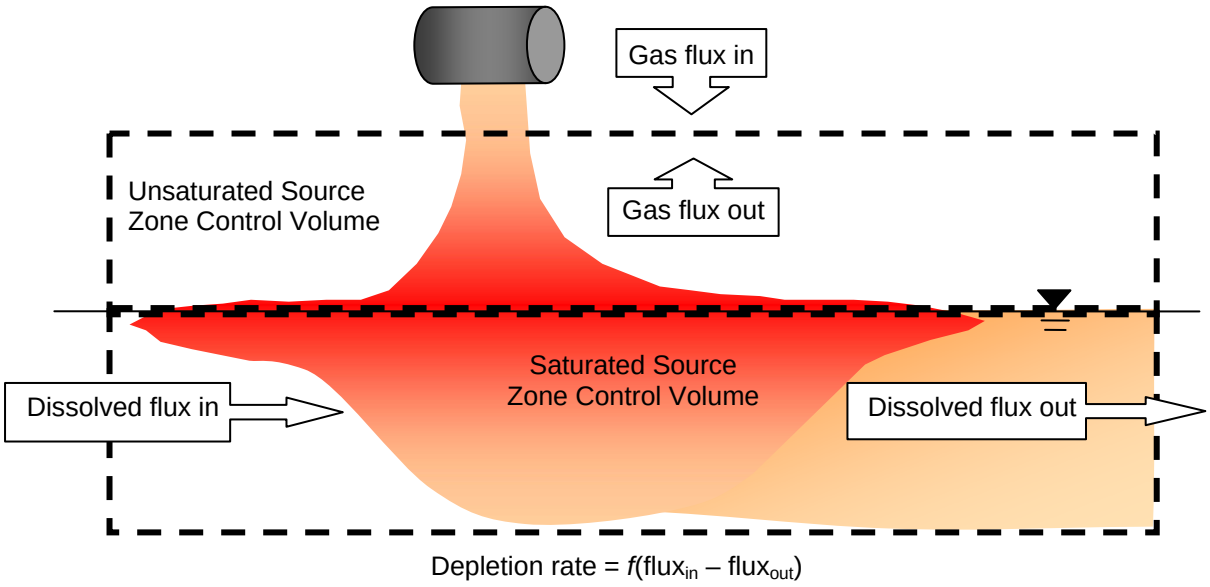

Figure 3-2. Example control volume "box" for quantitative assessment of NSZD.

Figure 3-3 summarizes the mass flux relationships of NSZD processes associated with dissolved LNAPL constituents.

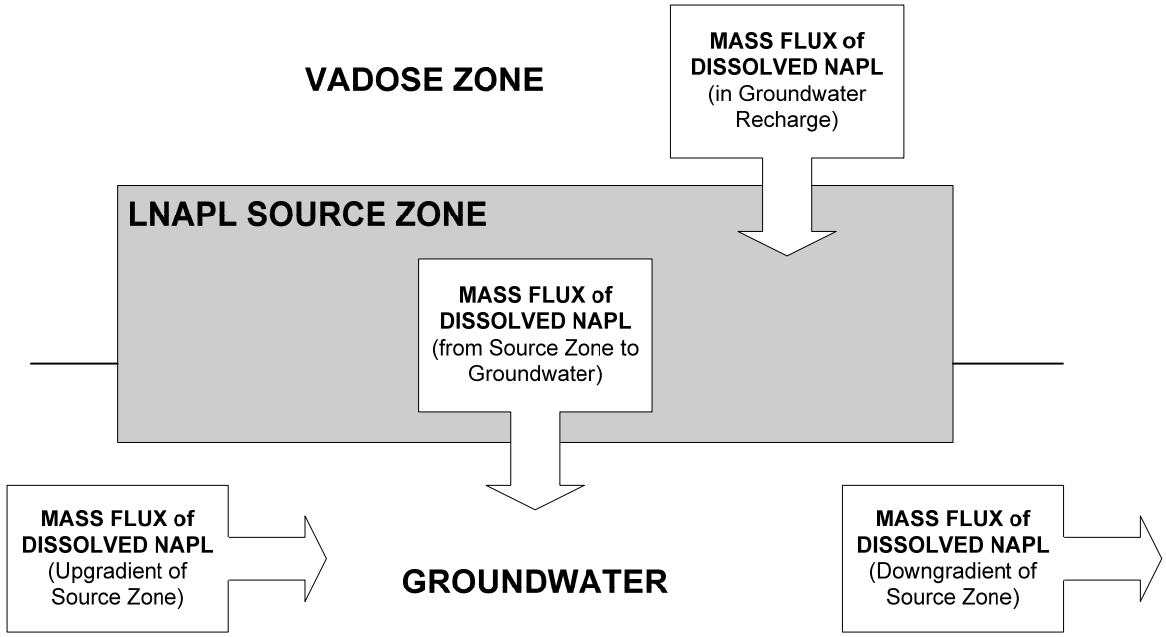

Figure 3-3. Mass flux diagram for dissolved LNAPL constituents.

In many cases, mass flux transfer of hydrocarbons via groundwater recharge and from upgradient groundwater is negligible, and the mass flux relationship is simplified to account for mass transfers occurring in only the *submerged* portion of the source zone (Figure 3-4).

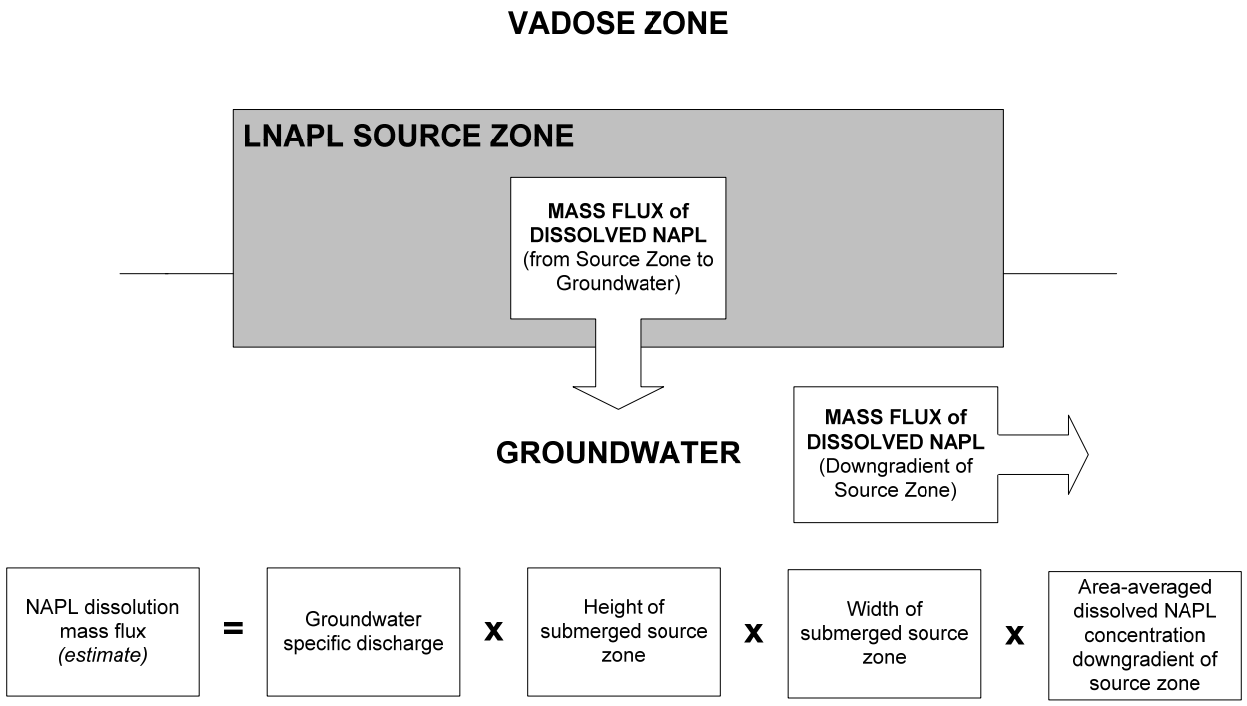

Figure 3-4. Simplified mass balance/mass flux for dissolved LNAPL constituents.

Mathematically, the *estimate* of the LNAPL dissolution mass flux using groundwater concentrations downgradient of source zone is shown in Equation 3-1:

$$R_{Dissoln} \approx q_d hw\langle C_d \rangle \qquad \textbf{[Eq. 3-1]}$$

where

q_d = groundwater specific discharge $\left(\frac{\text{m}^3\ \text{H}_2\text{O}}{\text{m}^2 \cdot \text{sec}}\right)$,

h = thickness of submerged source zone (m),

w = width of submerged source zone (m),

C_d = area-averaged groundwater concentration $\left(\frac{\text{kg } i}{\text{m}^3\ \text{H}_2\text{O}}\right)$.

3.5.3 Estimate of Dissolved-Phase Source Zone Mass Depletion Rate by Biodegradation

Figure 3-5 shows the mass balance relation for biodegradation of dissolved-phase source zone constituents.

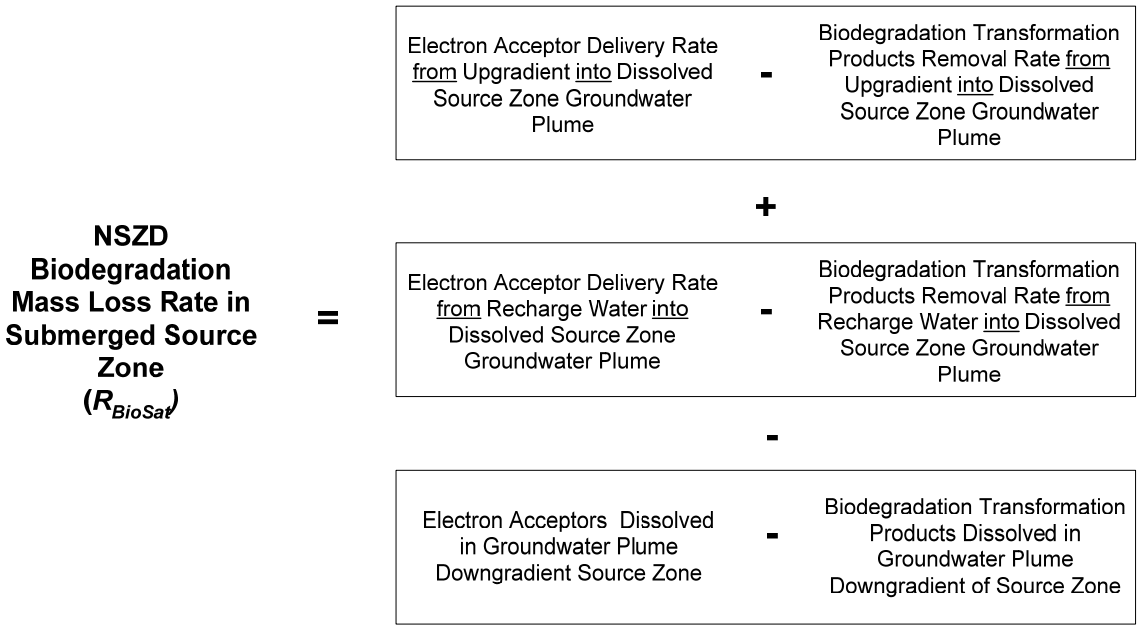

Figure 3-5. Mass balance relation for biodegradation of dissolved LNAPL constituents.

Mathematically, the mass loss rate estimate of source zone via biodegradation in the saturated zone is as shown in Equation 3-2:

$$R_{Bio-Sat} \approx \qquad \textbf{[Eq. 3-2]}$$

$$WHq_u\left\{\left[S_{O_2}\left\langle C_{O_2,u}\right\rangle\right]+\left[S_{NO_3^-}\left\langle C_{NO_3^-,u}\right\rangle\right]+\left[S_{SO_4^{2-}}\left\langle C_{SO_4^{2-},u}\right\rangle\right]-\left[S_{Fe^{2+}}\left\langle C_{Fe^{2+},u}\right\rangle\right]-\left[S_{Mn^{2+}}\left\langle C_{Mn^{2+},u}\right\rangle\right]-\left[S_{CH_4}\left\langle C_{CH_4,u}\right\rangle\right]\right\}$$

$$+$$

$$WLq_R\left\{\left[S_{O_2}\left\langle C_{O_2,R}\right\rangle\right]+\left[S_{NO_3^-}\left\langle C_{NO_3^-,R}\right\rangle\right]+\left[S_{SO_4^{2-}}\left\langle C_{SO_4^{2-},R}\right\rangle\right]-\left[S_{Fe^{2+}}\left\langle C_{Fe^{2+},R}\right\rangle\right]-\left[S_{Mn^{2+}}\left\langle C_{Mn^{2+},R}\right\rangle\right]-\left[S_{CH_4}\left\langle C_{CH_4,R}\right\rangle\right]\right\}$$

$$-$$

$$WHq_d\left\{\left[S_{O_2}\left\langle C_{O_2,d}\right\rangle\right]+\left[S_{NO_3^-}\left\langle C_{NO_3^-,d}\right\rangle\right]+\left[S_{SO_4^{2-}}\left\langle C_{SO_4^{2-},d}\right\rangle\right]-\left[S_{Fe^{2+}}\left\langle C_{Fe^{2+},d}\right\rangle\right]-\left[S_{Mn^{2+}}\left\langle C_{Mn^{2+},d}\right\rangle\right]-\left[S_{CH_4}\left\langle C_{CH_4,d}\right\rangle\right]\right\}$$

where

Electron acceptors:	Biodegradation transform products:
O_2	Fe^{2+}
NO_3^-	Mn^{2+}
SO_4^{2-}	CH_4

Stoichiometric coefficient of species *i*: $S_i = \dfrac{\text{kg HC}}{\text{kg } i}$ **[Eq. 3-3]**

Estimate of area-averaged dissolved concentration of species *i*:

$$\langle C_i \rangle = \frac{\text{kg } i}{\text{m}^3 \text{ H}_2\text{O}} \quad \textbf{[Eq. 3-4]}$$

Biodegradation of LNAPL in the saturated zone changes the concentrations of dissolved components such as oxygen, methane, nitrate, sulfate, iron, and manganese. Accordingly, measurement of these changes approximates the rate of saturated zone biodegradation. Using the control volume given in Figure 3-2 and mass balance relation in Figure 3-5, this rate can be calculated using Equation 3-2. Table 3-2 lists representative stoichiometric coefficient values for the equations. Although the values given are for biodegradation of a reference hydrocarbon constituent ($C_{10}H_{22}$), they are valid for a wide range of petroleum hydrocarbons. Also, the calculation based on electron acceptor flux is not constituent specific. In other words, the degraded hydrocarbons are unidentified.

Table 3-2. Representative stoichiometric coefficients (S_i) for biodegradation of a reference hydrocarbon constituent ($C_{10}H_{22}$)

Biodegradation process	Biodegradation component	Stoichiometric coefficient (S_i)
Aerobic biodegradation	O_2	0.29 kg-HC/kg-O_2
Nitrate reduction	NO_3^-	0.19 kg-HC/kg-NO_3^-
Iron reduction	Fe^{2+}	0.041 kg-HC/kg-Fe^{2+}
Sulfate reduction	SO_4^{2-}	0.19 kg-HC/kg-SO_4^{2-}
Manganese reduction	Mn^{2+}	0.083 kg-HC/kg-Mn^{2+}
Methanogenesis	CH_4	1.1 kg-HC/kg-CH_4

Source: Adapted from Johnson, Lundegard, and Liu 2006.

3.5.4 Source Zone Mass Depletion by Volatilization and Biodegradation in the Unsaturated Zone

In the unsaturated zone, LNAPL is subject to volatilization and biodegradation. In addition, anaerobic biodegradation of the source zone may generate methane gas, which then migrates upward through the vadose zone. Figure 3-6 is a generalized schematic showing the location of these processes.

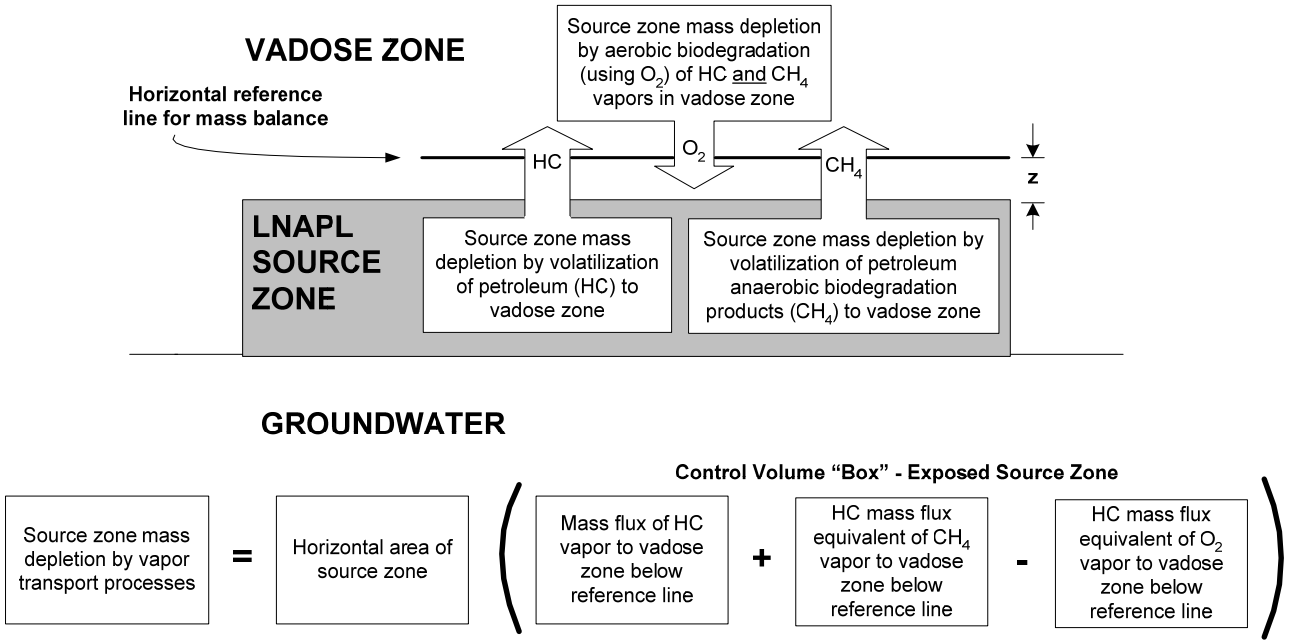

Figure 3-6. Reference diagram for NSZD mass depletion volatilization processes.

Table 3-3 summarizes additional site-specific source zone data necessary for completing quantitative NSZD assessments.

Table 3-3. Additional data needed for quantitative evaluation: Rates at which NSZD processes are occurring

Quantitative data	Purpose
Effective diffusion coefficients: measured (Johnson et al. 1998) or estimated (from soil moisture and total porosity, Millington and Quirk 1961)	Used with the Table 3-1, soil-gas profiles to estimate loss rates by volatilization and biodegradation (oxygen delivery and/or methane production rates)
Hydraulic conductivity values	Used with Table 3-1, dissolved concentration and groundwater elevation data to estimate loss rates by dissolution and biodegradation in the saturated zone

Source: Adapted from Johnson, Lundegard, and Liu 2006.

Hydrocarbon volatilization into the vadose zone generates a demand for oxygen. Commonly, the hydrocarbon vapors are subject to aerobic biodegradation, resulting in atmospheric oxygen diffusing downward towards the source zone. The resulting component flux or mass loss can be quantified by assuming a horizontal plane located above the source zone at a height (z) in Figure 3-6. Assuming that the downward diffusion or flux of atmospheric oxygen across the plane is caused by LNAPL biodegradation and that background oxygen demand and methane generation are negligible, the rate of component mass loss from the source area can be calculated using Equation 3a, given in Appendix C. The effective vapor phase diffusion coefficients required in Equation 3a may be measured using soil gas profiles (Johnson et al. 1998). Table 3-2 gives representative stoichiometric coefficients for aerobic biodegradation and methanogenesis.

Example Problem: Quantitative NSZD Assessment (Submerged LNAPL)

An instantaneous "snapshot" of the naturally occurring LNAPL source zone mass loss rate was calculated for the purpose of determining the current rate of NSZD as follows:

$$NSZD\ Rate = \text{Submerged NSZD rate} + \text{Exposed NSZD rate}$$

SUBMERGED NSZD RATE

The NSZD rate is calculated by summing the NAPL mass loss to dissolution in groundwater and the loss rate of dissolved mass biodegraded in groundwater, as follows:

$$\text{Submerged NSZD Rate} = \text{NAPL Mass Dissolution Rate} + \text{NAPL Dissolved Mass Biodegradation Rate}$$

The NAPL mass dissolution rate is calculated using Equation 3-1:

$$R_{Dissoln} \approx q_d hw\langle C_d \rangle$$

The LNAPL dissolved mass biodegradation rate is calculated using Equation 3-2. However, in this example problem, the mass added to the groundwater system via surface recharge is negligible and is not considered.

$$R_{Bio-Sat} \approx$$
$$WHq_u \left\{ \left[S_{O_2} \left\langle C_{O_2,u} \right\rangle \right] + \left[S_{NO_3^-} \left\langle C_{NO_3^-,u} \right\rangle \right] + \left[S_{SO_4^{2-}} \left\langle C_{SO_4^{2-},u} \right\rangle \right] - \left[S_{Fe^{2+}} \left\langle C_{Fe^{2+},u} \right\rangle \right] - \left[S_{Mn^{2+}} \left\langle C_{Mn^{2+},u} \right\rangle \right] - \left[S_{CH_4} \left\langle C_{CH_4,u} \right\rangle \right] \right\}$$
$$-$$
$$WHq_d \left\{ \left[S_{O_2} \left\langle C_{O_2,d} \right\rangle \right] + \left[S_{NO_3^-} \left\langle C_{NO_3^-,d} \right\rangle \right] + \left[S_{SO_4^{2-}} \left\langle C_{SO_4^{2-},d} \right\rangle \right] - \left[S_{Fe^{2+}} \left\langle C_{Fe^{2+},d} \right\rangle \right] - \left[S_{Mn^{2+}} \left\langle C_{Mn^{2+},d} \right\rangle \right] - \left[S_{CH_4} \left\langle C_{CH_4,d} \right\rangle \right] \right\}$$

Table C summarizes the NAPL groundwater mass dissolution and biodegradation data and calculations using the site data. The instantaneous NAPL mass depletion rates are presented on a daily and an annualized basis.

TABLE C

Submerged NAPL Source Zone Depletion Rate

	Well Number	TPH-GRO (C_{10})
Downgradient Wells	MW-3	3.000 mg/L
	MW-4	4.000 mg/L
Upgradient Wells (Median)	MW-16	ND
	MW-17	ND

Electron Acceptors (Median)			Biodegradation Transform. Products		
Oxygen (mg/L O_2)	Nitrate (mg/L NO_3^-)	Sulfate (mg/L SO_4^{2-})	Iron (mg/L Fe^{2+})	Manganese (mg/L Mn^{2+})	Methane (mg/L CH_4)
0.5 mg/L	0.0 mg/L	10.0 mg/L	16.0 mg/L	1.0 mg/L	4.5 mg/L
5.0 mg/L	4.2 mg/L	40.0 mg/L	0.00 mg/L	0.0 mg/L	0.000 mg/L
0.29 kg HC/kg O_2	0.19 kg HC/kg NO_3^-	0.19 kg HC/kg SO_4^{2-}	0.041 kg HC/kg Fe^{2+}	0.083 kg HC/kg Mn2+	1.1 kg HC/kg CH_4
Stoichiometric Coefficients (for $C_{10}H_{22}$ equivalent)					

NAPL specific gravity	NAPL SG =	0.75
Hydraulic gradient (m/m)	$^{dh}/_{dl}$ =	0.0010 m/m
Hydraulic conductivity (cm/s)	K =	3.0E-3 cm/sec
Average thickness of ground-water	H =	244.00 cm
Average width of groundwater plume	W =	3300.00 cm

Submerged NAPL Mass Dissolution Rate		
Area-averaged dissolved TPH concentration (downgradient) (mg/L)	$\langle C_d \rangle$ =	3.500 mg/L
Groundwater specific discharge (apparent velocity)	q_d =	2.6E-1 cm/day
Estimate of NAPL mass dissolution rate (kg - HC/day)	$R_{Dissoln}$ =	7.30E-4 kg HC/day

Submerged NAPL Mass Biodegradation Rate		
Estimate of dissolved NAPL mass depletion via biodegradation	$R_{Bio-Sat}$ =	2.82E-3 kg HC/day

Submerged NAPL Total Mass Depletion Rate		
Estimated total submerged NAPL mass depletion rate	$R_{Submerged}$ =	1.29E+0 kg HC/yr
	$R_{submerged}$ =	4.55E-1 gal HC/yr

Several factors should be considered when selecting the location of the horizontal reference plane depicted in Figure 3-6. One factor is the presence of significant background oxygen demand and/or methane generation. In this case, optimal placement of the plane would be immediately above the source area. Finally, effective vapor phase diffusion coefficients as required by Equations 3a and 3b (see Appendix C) are difficult to measure in the capillary zone. Accordingly, placement of the plane in the capillary zone could introduce significant error in the equations (see Example Case Study, Appendix A, Section A.3.3).

The source zone mass depletion rate comprising the various vapor phase transport and biodegradation processes, as represented in Figure 3-6, is estimated as shown in Equation 3-5.

$$R_{Vapor} \approx WL\left\{-D_{HC}(C_{HC})_z - S_{CH_4}D_{CH_4}(C_{CH_4})_z + S_{O_2}D_{O_2}(C_{O_2})_z\right\} \qquad \textbf{[Eq. 3-5]}$$

Amos and Mayer (2006) and Amos et al. (2005) reported that methane produced by anaerobic biodegradation of submerged LNAPL can be entrapped as bubbles in the saturated zone. The methane bubbles can escape into the overlying vadose zone by ebullition and contribute to the observed soil vapor methane concentration. In such cases, the exposed LNAPL source zone mass depletion rate determined using Equation 3-5 may actually include some mass depletion occurring in the submerged LNAPL source zone (thus, overestimating the exposed source zone mass depletion rate).

Example Problem: Quantitative NSZD Assessment (Exposed NAPL)

EXPOSED NSZD RATE

The exposed NSZD rate is calculated using Equation 3-5:

$$R_{Vapor} \approx WL\left\{-D_{HC}(C_{HC})_z - S_{CH_4}D_{CH_4}(C_{CH_4})_z + S_{O_2}D_{O_2}(C_{O_2})_z\right\}$$

However, in this example problem, only the oxygen diffusivity rate is known (facilitating the placement of the control plane). Therefore, Equation 3-5 is simplified to the following:

$$R_{Vapor} \approx WL\left\{S_{O_2}D_{O_2}(C_{O_2})_z\right\}$$

4. EVALUATION OF LONG-TERM NATURAL SOURCE ZONE DEPLETION

Numerous aspects of NSZD projects can be evaluated for the purpose of determining their long-term progress. Long-term NSZD evaluations discussed in this section include (a) establishing NSZD baseline conditions, (b) determining relative efficacies of NSZD processes, (c) monitoring changes in potential risks of NSZD, and (d) predicting NSZD progress. These measured and predicted NSZD performance metrics are essential elements of a comprehensive demonstration for an NSZD project proposal.

4.1 Determining Source Zone LNAPL Composition

Source zone LNAPL composition determinations are fundamental to establishing NSZD baseline conditions and should be accomplished as early as possible. The LNAPL baseline compositions can then be used in comparisons with subsequent measurements to evaluate the magnitude and type of changes to the source zone that may have occurred.

Selection of Appropriate LNAPL Fractions

TPH-based LNAPLs comprise complex mixtures of many chemical constituents (e.g., TPHCWG 1998). While it is important to characterize the source zone with as much detail as possible, NSZD evaluations may be based on fewer, more diagnostic, reference constituents. The analysis of magnitudes and trends of just a few appropriately selected constituents can provide a robust, long-term NSZD evaluation with minimal laboratory analytical demands.

For example, evaluations of NSZD processes in the saturated zone (Section 2.2) may be based on TPH fractions with high aqueous solubility. Since such constituents possess a greater propensity to dissolve in groundwater, they are likely to be the most sensitive indicators capable of demonstrating that mass transfer process. Similarly, TPH fractions with greatest volatility (e.g., vapor pressure) may be used as references in the vadose zone for LNAPL volatilization to soil gas (see Section 2.1). Additionally, LNAPL fractions with high toxicities may be used as reference constituents when evaluating potential health risks associated with progress of an NSZD project (see Section 4.3). TPHCWG (1997) provides additional discussion selection criteria for TPH reference constituents.

Over time, as certain TPH fractions are preferentially depleted from the source zone based on their physical and/or chemical properties, the remaining LNAPL composition will change as the residual constituents become relatively enriched compared to the depleted ones. Such changes in composition are persuasive evidence for the activity of NSZD processes and should be discussed in NSZD demonstrations.

4.2 Evaluating Relative Efficacies of NSZD Processes

A combination of NSZD processes may be occurring simultaneously within an LNAPL source zone setting (Sections 2.1–2.3). Source zones present with both an exposed portion in the vadose zone and a submerged portion in the saturated zone are likely undergoing depletion by different NSZD processes at different mass depletion rates. NSZD evaluations for sites at which different NSZD processes are occurring simultaneously can include (a) an accounting of NSZD process-based mass loss rates and (b) a comparison of NSZD mass loss rates between the exposed source zone and the submerged source zone.

Estimates of site-wide source zone mass depletion rates may be obtained using techniques described in Sections 3.5.2 and 3.5.3 (for the submerged source zone) and Section 3.5.4 (for the exposed source zone). Current estimates of the different mass depletion rates throughout the source zone can be used to distinguish areas of the source zone that are undergoing relatively rapid mass depletion and those that are not. A full accounting of mass depletion rates throughout the source zone should be included in NSZD demonstrations. Additionally, spatial distributions

of mass depletion rate estimates throughout the source zone are useful in numerical modeling of NSZD processes (Section 4.5).

The comparison of mass depletion rates to remaining source zone mass provides useful information for demonstrating NSZD effectiveness. Mass depletion rates in the exposed source zone (primarily by gas transport) can be compared to the residual mass of the volatile TPH fraction to estimate the potential of NSZD to meet a remedial goal in the exposed source zone. Similarly, the mass depletion rate in the submerged source zone (primarily by dissolution to groundwater) can be compared to the residual mass of the soluble TPH fraction.

4.3 Evaluating Risks Associated with NSZD Processes

NSZD processes comprise the transfer of constituent mass from a phase in the source zone to a phase in an environmental medium. Once transferred to an environmental medium, the source zone constituent is subject to biotic and abiotic destruction and ultimate removal. However, since rates of destruction vary greatly from site to site, the residence times of source zone constituents in environmental media can vary greatly. If the residence time of source zone constituents in environmental media is high, then much more time is available for the constituents to migrate to a human or ecological receptor. Therefore, an evaluation should be conducted of the potential for impact by source zone constituents to human health and ecological receptors. The highest potential impacts to receptors are primarily from groundwater transport of dissolved-phase constituents from the submerged source zone and gas-phase transport of volatilized constituents from the exposed source zone.

4.3.1 Potential Risks of Groundwater Impacts

The transport of constituents dissolved from a submerged source zone and transported via groundwater presents potential risks to human health and ecology. ASTM Standard Guide E1739 (ASTM 2002) summarizes potential risks associated with fate and transport of dissolved-phase constituents in groundwater. Included therein are (a) the potential for impact of a potable water supply receptor and the risk associated with groundwater ingestion and (b) the potential for impact of indoor and/or outdoor ambient air via volatilization of dissolved-phase constituents and the risk associated with air inhalation. These potential risks can be addressed using look-up values or fate and transport modeling calculations (e.g., ASTM E1739). Alternatively, more advanced modeling efforts can be performed (Section 4.5).

4.3.2 Potential Risks of Vapor Impacts

The transport of constituents volatilized from an exposed source zone and transported in the gas phase through the subsurface presents potential risks to human health and ecology. ASTM E1739 and ITRC (2007b) summarize potential risks associated with fate and transport of constituents volatilized into the vadose zone. Included therein is the potential for impact to indoor and/or outdoor ambient air via volatilization of exposed source zone LNAPL and the risk associated with air inhalation. These potential risks can be addressed using look-up values or fate and transport modeling calculations (e.g., ASTM E1739). Alternatively, more advanced modeling efforts can be performed (see Section 4.5).

4.4 Evaluating Long-Term Behavior

The long-term behavior of source zone mass loss can be evaluated for both the submerged and exposed portions of the source zone. The following sections describe laboratory methodologies that have been developed into bench-scale tests to facilitate such an evaluation. The bench-scale tests are laboratory experiments and not standard laboratory analyses.

4.4.1 Bench-Scale Test for Long-Term Source Mass Loss by LNAPL Dissolution

Long-term mass loss from the submerged LNAPL source zone by dissolution to groundwater can be estimated from short-term bench-scale weathering tests. Liu (2004) describes an experimental procedure by which a serial sequential batch equilibrium approach can approximate accelerated weathering. The results of the accelerated weathering experiments provide information on changes in LNAPL chemistry, mass loss, and dissolved-phase constituent concentrations. Each short-term bench-scale batch experiment can be related to long-term field conditions in the following relation:

LABORATORY TIME		FIELD TIME
Mass of NAPL source dissolved in cumulative volume of water during experiment	α	Mass of NAPL source zone dissolved in cumulative volume of groundwater moving past source at known groundwater velocity

Mathematically, the laboratory scale is related to the field scale by Equation 4-1:

$$t_{field} = \frac{V_{lab}}{V_{o,lab}} \times \frac{LnS}{q} \qquad \textbf{[Eq. 4-1]}$$

where

t_{field} = field-scale time,
V_{lab} = volume water contacted LNAPL,
$V_{o,lab}$ = volume LNAPL,
L = length of source zone in direction of groundwater flow,
n = source zone porosity,
S = fraction of LNAPL pore space saturation in source zone,
q = groundwater specific discharge through source zone porosity.

4.4.2 Bench-Scale Test Long-Term Source Mass Loss by LNAPL Volatilization

Long-term mass loss from the exposed LNAPL source zone by volatilization to the vadose zone (as soil gas) may be estimated from short-term, bench-scale weathering tests. Liu (2004) describes an experimental procedure by which an inert gas is passed through a reaction cell at a rate that allows equilibrium volatilization of LNAPL. The equilibrium LNAPL vapor concentration that is entrained in the inert gas flow is measured as it exits the reaction cell.

LABORATORY TIME		FIELD TIME
Mass removal of NAPL source by equilibrium volatilization via accelerated transfer from reaction cell by inert gas flow	α	Mass removal from NAPL source zone by equilibrium volatilization and diffusive migration through vadose zone soil column

Mathematically, the laboratory scale is related to the field scale by Equation 4-2:

$$t_{field} = t_{lab} \cdot \frac{Q\delta SnH}{D^{eff} V_{L,O}} \qquad \textbf{[Eq. 4-2]}$$

where

t_{field} = field-scale time
t_{lab} = lab-scale time,
Q = vapor flow rate,
δ = approximate depth to source zone,
S = fraction of LNAPL pore space saturation in source zone,
n = source zone porosity,
H = source zone thickness,
D^{eff} = bulk effective air diffusivity in field,
$V_{L,0}$ = initial LNAPL volume used in bench test.

Table 4-1. Data needed to assess longer-term effects of NSZD

Assessment data	Purpose
Chemical analyses of hydrocarbon composition in soils at different depths at sites with historical spills (>10 years old)	Reveal vertical weathering profiles and patterns; shallow samples (most weathered) vs. deeper samples (least weathered); at and around capillary fringe: upgradient samples (more rapid weathering) vs. downgradient samples (less weathering)
Laboratory leaching tests conducted on naturally weathered soil samples	To assess how weathering might affect groundwater impacts; headspace analyses on these samples could also provide information on potential effects and impacts via vapor migration pathways
Short-term (weeks to months) bench-scale accelerated weathering tests	Designed to simulate the effects of hundreds of years of natural weathering processes (Liu 2004); these could incorporate laboratory leaching tests to help assess how long-term weathering may affect groundwater impacts
Quantification of limiting biodegradation reactants, identification of limiting processes and factors, etc.	Assessment of the extent to which loss processes are sustainable

Source: Adapted from Johnson, Lundegard, and Liu 2006.

4.5 Modeling of NSZD Processes

The quantitative evaluation of NSZD (see Section 3.5) may need to be supplemented by computational models representing one or more specific NSZD processes. Modeling of site-specific NSZD processes can be useful to (a) facilitate the understanding of the site-specific significance of one or more processes on overall NSZD rates, (b) evaluate the potential effectiveness of NSZD as a stand-alone remedial option, (c) predict evolution of source zone behavior and estimate NSZD remedial time frames, and (d) provide a basis for NSZD remedy demonstrations. This section describes various options for more detailed modeling of NSZD processes and summarizes available models and potential modeling techniques.

4.5.1 Use of Models for NSZD Remediation Predictions

When applied properly, models can be useful in predicting the behavior of NSZD systems. Rates of source zone mass depletion due to mass transfer and biodegradation at a time in the future can be estimated. The distribution of source zone mass in a multimedia system can be quantified for a time in the future. Progress of a NSZD remedy can be tracked through time, and a time frame for meeting a remediation goal can be estimated.

NOTE: The predictive modeling methodologies described in this section are based mostly on *equilibrium* calculations. The use of equilibrium calculations contrasts with the empirical, "instantaneous," site-specific determination of NSZD rates described in the previous sections.

4.5.2 Use of Models in NSZD Demonstrations

Model results can be used in demonstrations to support NSZD evaluations. This topic is discussed further in a forthcoming technical/regulatory guidance document, *Evaluating LNAPL Remedial Technologies for Achieving Project Goals*, which the ITRC LNAPLs Team is developing concurrently with this document.

4.5.3 Use of Models in Evaluating NSZD Risks

Modeling of NSZD processes and the resulting redistribution of mass can be useful in evaluations of collateral risks that might be generated during the source zone evolution. Fate and transport modeling of NSZD volatilization and biodegradation processes associated with exposed source zones can be used to predict expected vapor-phase constituent concentrations of LNAPL components in ambient air for comparison with allowable regulatory levels. Similarly, fate and transport modeling of NSZD dissolution and biodegradation processes in groundwater can be used to predict future dissolved-phase plume dynamics and concentrations for comparison to regulatory requirements at applicable points of compliance. NSZD modeling results that indicate the potential for excess risk along an exposure pathway can be used to anticipate the risk and modify the proposed NSZD plan to mitigate it. Evaluations of NSZD risks should be included in NSZD demonstrations.

4.5.4 NSZD Model Parameters

Modeling of NSZD processes is complicated by the large number of associated variables (e.g., Miller, Poirier-McNeill, and Mayer 1990). Consequently, the numerous software packages that are currently available to evaluate NSZD system behavior are designed to perform model calculations differently and may have different capabilities. Additionally, different models are designed to answer different questions in different ways. This section describes some model parameters that are applicable to NSZD behavior. Table 4-2 summarizes the NSZD-related capabilities of the various models.

- **Model Type.** The different model packages typically perform calculations in one of several ways. Some models use an analytical solution; others use a numerical method. Some models calculate a one-dimensional result, while others can generate two- and three-dimensional results. Some model packages described here are stand-alone NSZD-process specific, while others are numeric engines which may require coupling to another software package.

- **LNAPL Mobility.** LNAPL residual saturations and LNAPL mobility can be simulated to estimate time frames for source zone to reach hydraulic equilibrium. Some models can simulate smear zone dynamics associated with changing water table elevations.

- **LNAPL Dissolution.** LNAPL dissolution into groundwater (see Section 3.5.2) can be simulated using calculations for single- or multi-component LNAPL. Dissolution mass flux predictions, component transfer rates at different times, and evolution of depletion of a submerged source zone are possible with certain models.

- **LNAPL Volatilization.** LNAPL volatilization to the vadose zone (see Section 3.5.4) can be simulated using calculations for single- or multi-component LNAPL volatilization. Volatilization mass flux and transfer rates for each component at different times and describe evolution of depletion of an exposed source zone are possible with some models.

- **Groundwater Fate and Transport.** Some models can be used to simulate the fate and transport of dissolved-phase plumes originating from LNAPL dissolution of a submerged source. The fate and transport simulations can be calculated in one-, two- or three-dimensional mode and use the transient and/or steady state solutions.

- **LNAPL Recovery.** The effects of LNAPL recovery on the evolution of source zone depletion can be estimated by some models. Simulations of LNAPL recovery can include the use of different technologies implemented for varying periods of time with varying recovery rates and/or cumulative mass recovered. Some models can couple LNAPL recovery with NSZD processes to facilitate the appropriate design of effective source zone remedies.

- **Biodegradation.** The effects of biodegradation on the dissolved-phase plume originating from a submerged source zone (see Section 3.5.3) and/or the effects of biodegradation on vapors from an exposed source (see Section 3.5.4) can be simulated.

Table 4-2. Summary of NSZD-related model capabilities

Model	Type	NSZD-related model parameters						References
		LNAPL mobility	LNAPL dissolution	LNAPL volatilization	Groundwater fate and transport	LNAPL recovery	Biodegradation	
API-LNAST	Analytical	YES—Predicts time of source zone to reach mobility equilibrium	YES—Predicts component(s) mass flux to groundwater	YES—Predicts component(s) vapor flux w/vertical diffusion	YES—1-D analytical w/3-D dispersion	YES—Predicts hydraulic recovery of different type systems	YES—Pseudo-first-order biodecay half-life	API 2002, 2004
BIONAPL/3D	3-D finite element w/flow, LNAPL dissolution, and biodegradation	NO—Assumes LNAPL at residual saturation	YES—Rate-limited or equilibrium dissolution	NO	YES—3-D flow; multicomponent (gasoline) reactive mass transport	NO	YES—Multiple electron acceptors and microbial populations	Molson 2002
PHT3D	PHREEQC-2 coupled w/finite difference flow model and transport simulator; accommodates variety of transport and reaction modes	NO	YES	NO	YES—Multicomponent reactive transport; kinetic and equilibrium reactions	NO	YES—Microbial growth and decay; sequential reactive decay; kinetic decay	Prommer 2006
RT3D	3-D mass transport numerical engine (solver)	NO—Assumes LNAPL is immobile	YES—Rate transfer at equilibrium dissolution	NO	YES—Multicomponent reactive transport; kinetic and equilibrium reactions	NO	YES—Sequential reactive decay; kinetic decay	Clement 1997
SourceDK	Spreadsheet-based	NO	YES	NO	YES—1-D analytical	NO—Accelerated LNAPL dissolution by groundwater pumping	YES—Multi-component first-order biodecay	AFCEE 2004

5. REFERENCES

AFCEE (Air Force Center for Environmental Excellence). 2003. *Light Nonaqueous-Phase Liquid Weathering at Various Fuel Release Sites* (2003 update). Prepared by Parsons Engineering Science, Inc., Brooks City Base, San Antonio, Tex.

AFCEE. 2004. *SourceDK Remediation Timeframe Decision Support System Version 1.0.* San Antonio, Tex.: Brooks City Base Technology Transfer Division.

Alexander, M. 1977. *Introduction to Soil Microbiology*, 2nd ed. New York: Wiley & Sons.

Amos, R. T., and K. U. Mayer. 2006. Investigating the Role of Gas Bubble Formation and Entrapment in Contaminated Aquifers: Reactive Transport Modeling," *Journal of Contaminant Hydrology* **87**: 123–54.

Amos, R. T., K. U. Mayer, B. A. Bekins, G. N. Delin, and R. L. Williams. 2005. "Use of Dissolved and Vapor-Phase Gases to Investigate Methanogenic Degradation of Petroleum Hydrocarbon Contamination in the Subsurface," *Water Resources Research* **41**(2): W02001.

API (American Petroleum Institute). 2002. *Evaluating Hydrocarbon Removal from Source Zones and Its Effect on Dissolved Plume Longevity and Magnitude.* Publication 4715. Regulatory Analysis and Scientific Affairs Department. Washington, D.C.: API Publishing Services.

API. 2004. *API Interactive LNAPL Guide Version 2.0.3.* Soil and Groundwater Technical Task Force, Washington, D.C.

ASTM 2002. *Standard Guide for Risk-Based Corrective Action Applied at Petroleum Release Sites.* E1739. Book of Standards, vol. 11.05.

Atlas, R. M. 1981. "Microbial Degradation of Petroleum Hydrocarbons: An Environmental Perspective," *Microbiological Reviews* **45**(1): 180–209.

Baedecker, M. J., I. M. Cozzarelli, R. P. Eganhouse, D. I. Siegel, and P. C. Bennett. 1993. "Crude Oil in a Shallow Sand And Gravel Aquifer: III. Biogeochemical Reactions and Mass Balance Modeling in Anoxic Groundwater," *Applied Geochemistry* **8**: 569.

Baedecker, M. J., I. M. Cozzarelli, J. R. Evans, and P. P. Hearn. 1992. "Authigenic Mineral Formation in Aquifers Rich in Organic Material," in *Water-Rock Interaction*, vol. 2, Y. K. Kharaka and A. S. Maest, eds. Rotterdam, The Netherlands: A. A. Balkema.

Barker, J. F., G. C. Patrick, and D. Major. 1987. "Natural Attenuation of Aromatic Hydrocarbons in a Shallow Sand Aquifer," *Groundwater Monitoring Review* **7**(1): 64–71.

BEG (Bureau of Economic Geology). 1997. *Extent, Mass, and Duration of Hydrocarbon Plumes from Leaking Petroleum Storage Tanks Sites in Texas*. Geological Circular 97-1. Austin, Tex.: University of Texas Bureau of Economic Geology.

Bekins, B. A., I. M. Cozzarelli, E. M. Godsy, E. Warre, H. I. Essaid, and M. E. Tucillo. 2001. "Progression of Natural Attenuation Processes at a Crude Oil Spill Site: II. Controls on Spatial Distribution of Microbial Populations," *Journal of Contaminant Hydrology* **53**(3–4): 387–406.

Bekins, B. A., F. D. Hostettler, W. N. Herkelrath, G. N. Delin, E. Warren, and H. I Essaid. 2005. "Progression of Methanogenic Degradation of Crude Oil in the Subsurface," *Environmental Geosciences* **12**: 139–52.

Bennett, P. C., D. E. Siegel, M. J. Baedecker, and M. F. Hult. 1993. "Crude Oil in a Shallow Sand and Gravel Aquifer: 1. Hydrogeology and Inorganic Geochemistry," *Applied Geochemistry* **8**: 529.

Birman, I., and M. Alexander. 1996. "Effect of Viscosity of Nonaqueous-Phase Liquids (NAPLs) on Biodegradation of NAPL Constituents," *Environmental Toxicology and Chemistry* **15**(10): 1683–86.

Bockelmann A., T. Ptak, and G. Teutsch. 2001. "An Analytical Quantification of Mass Fluxes and Natural Attenuation Rate Constants at a Former Gas Works Site, *Journal of Contaminant Hydrology* **53**(3–4): 429–53.

Borden, R. C., C. A. Gomez, and M. T. Becker. 1995. "Geochemical Indicators of Intrinsic Bioremediation," *Journal of Groundwater* **33**(2): 180.

Bouwer, E. J., and P. L. McCarty. 1984. "Modeling of Trace Organics Biotransformation in the Subsurface," *Groundwater* **22**: 433.

Chiang, C. Y., J. P. Salanitro, E. Y. Chai, J. D. Colthart, and C. L. Klein. 1989. "Aerobic Biodegradation of Benzene, Toluene, and Xylene in a Sandy Aquifer—Data Analysis and Computer Modeling," *Journal of Groundwater* **27**(6): 823.

Clement, T. P. 1997. *RT3D: A Modular Computer Code for Simulating Reactive Multi-Species Transport in 3-Dimensional Groundwater Systems.* PNNL-SA-11720. Richland, Wash.: Pacific Northwest National Laboratory.

Cozzarelli, I. M., and M. J. Baedecker. 1992. "Oxidation of Hydrocarbons Coupled to Reduction of Inorganic Species in Groundwater," in *Water-Rock Interaction*, vol. 1, *Low-Temperature Environments*, Y. K. Kharaka and A. S. Maest, eds. Brookfield, Mass.: A. A. Balkema.

Cozzarelli, I. M., M. J. Baedecker, R. P. Eganhouse, and D. F. Goerlitz. 1994. "The Geochemical Evolution of Low-Molecular-Weight Organic Acids Derived from the Degradation of Petroleum Contaminants in Groundwater," *Geochimica Cosmochimica Acta* **58**: 863.

Cozzarelli, I. M., R. P. Eganhouse, and M. J. Baedecker. 1990. "Transformation of Monoaromatic Hydrocarbons to Organic Acids in Anoxic Groundwater Environment," *Environmental Geology and Water Science* **16**: 135.

Daniel, D. E. 1993. *Geotechnical Practice for Waste Disposal.* New York: Chapman and Hall.

DeVaull, G. E., R. A. Ettinger, and J. B. Gustafson. 2002. "Chemical Vapor Intrusion from Soil or Groundwater to Indoor Air: Significance of Unsaturated Zone Biodegradation on Aromatic Hydrocarbons," *Soil and Sediment Contamination* **11**: 625–41.

DeVaull, G. E., R. A. Ettinger, J. P. Salanitro, and J. B. Gustafson. 1997. "Benzene, Toluene, Ethylbenzene and Xylenes [BTEX] Degradation in Vadose Zone Soils During Vapor Transport: First-Order Rate Constants," pp. 365–79 in *Proceedings of the NGWA/API Petroleum Hydrocarbon and Organic Chemicals in Groundwater Conference*, Houston.

Douglas, G. S., K. J. McCarthy, D. T. Dahlen, J. A. Seavy, W. G. Steinhauer, R. C. Prince, and D. L. Elmendorf. 1992. "The Use of Hydrocarbon Analyses for Environmental Assessment and Remediation," pp. 1–21 in *Contaminated Soils: Diesel Fuel Contamination*, P. T. Kostecki and E. J. Calabrese, eds. Chelsea, Mich.: Lewis Publishers.

Efroymson, R. A., and M. Alexander. 1991. "Biodegradation by an *Arthobacter* Species of Hydrocarbons Partitioned into an Organic Solvent," A*pplied Environmental Microbiology* **57**: 1441–47.

Efroymson, R. A., and M. Alexander. 1994a. "Biodegradation in Soil of Hydrophobic Pollutants in Nonaqueous-Phase Liquids (NAPLs)," *Environmental Toxicology and Chemistry* **13**(3): 405–11.

Efroymson, R. A. and M. Alexander. 1994b. "Role of Partitioning in Biodegradation of Phenanthrene Dissolved in Nonaqueous-Phase Liquids, *Environmental Science and Technology* **28**(6): 1172–79.

Eganhouse, R. P., M. J. Baedecker, I. M. Cozzarelli, G. R. Aiken, K. A. Thorn, and T. F. Dorsey. 1993. "Crude Oil in a Shallow Sand and Gravel Aquifer: 2. Organic Geochemistry," *Applied Geochemistry* **8**: 551.

EPA (Environmental Protection Agency). 1987. *Processes Affecting Subsurface Transport of Leaking Underground Tank Fluids*. Las Vegas: Environmental Monitoring Systems Laboratory, Office of Research and Development.

EPA. 1995. *Light Nonaqueous-Phase Liquids*. EPA/540/S-95/500. EPA Groundwater Issue.

EPA. 1996. *Bioscreen Natural Attenuation Support System User's Manual.* EPA/600/R-96/087.

Falta, R., and N. Bulsara. 2004. "Lead Scavengers: A Leaded Gasoline Legacy?" *L.U.S.T.Line Bulletin* **47**: 6–10.

Farr, A. M., R. J. Houghtalen, and D. B. McWhorter. 1990. "Volume Estimation of Light Nonaqueous Phase Liquids in Porous Media," *Ground Water* **28**: 48–56.

Gaganis, P., P. Kjeldsen, and V. N. Burganos. 2004. "Modeling Natural Attenuation of Multicomponent Fuel Mixtures in the Vadose Zone: Use of Field Data and Evaluation of Biodegradation Effects," *Vadose Zone Journal* **3**: 1262–75.

Gelhar, L. W., C. Welty, and K. R. Rehfeldt. 1992. "A Critical Review of Data on Field-Scale Dispersion in Aquifers," *Water Resources Research* **28**: 1955–74.

Hostettler, F. D., Y. Wang, Y. S. Huang, W. H. Cao, B. A. Bekins, C. E. Rostad, C. F Kulpa, and A. Laursen. 2007. "Forensic Fingerprinting of Oil-Spill Hydrocarbons in a Methanogenic Environment—Mandan, ND and Bemidji, MN," *Environmental Forensics* **8**: 139–53.

Huntley, D., R. N. Hawk and H. P. Corley. 1994. "Nonaqueous-Phase Hydrocarbon in a Fine-Grained Sandstone: 1. Comparison Between Measured and Predicted Saturations and Mobility," *Ground Water* **32**: 626–34.

Inoue, A., and K. Horikoshi. 1991. "Estimation of Solvent-Tolerance of Bacteria by the Solvent Parameter log P," *Journal of Fermentation and Bioengineering* **71**(3): 194.

ITRC (Interstate Technology & Regulatory Council). 2007a. *Vapor Intrusion Pathway: A Practical Guideline*. VI-1. Washington, D.C.: Interstate Technology & Regulatory Council, Vapor Intrusion Team. www.itrcweb.org.

ITRC. 2007b. *Vapor Intrusion Pathway: Investigative Approaches for Typical Scenarios (A Supplement to VI-1)*. VI-1A. Washington, D.C.: Interstate Technology & Regulatory Council, Vapor Intrusion Team. www.itrcweb.org.

ITRC. 2007c. *Triad Implementation Guide*. SCM-3. Washington, D.C.: Interstate Technology & Regulatory Council; Sampling, Characterization, and Monitoring Team. www.itrcweb.org.

Johnson, P. C., C. Bruce, R. L. Johnson, and M. W. Klemblowski. 1998. "In Situ Measurement of Effective Vapor-Phase Porous Medium Diffusion Coefficients," *Environmental Science and Technology* **32**(21): 3405–09.

Johnson, P. C., P. Lundegard, and Z. Liu. 2006. "Source Zone Natural Attenuation at Petroleum Hydrocarbon Spill Sites: I. Site-Specific Assessment Approach," *Ground Water Monitoring and Remediation* **26**: 82–92.

Kanaly, R. A., R. Bartha, K. Watanabe, and S. Harayama. 2000. "Rapid Mineralization of Benzo[a]pyrene by a Microbial Consortium Growing on Diesel Fuel," *Applied and Environmental Microbiology* **66**(10): 4205–11.

Klenk, I. D, and Grathwohl, P. 2002. "Transverse Vertical Dispersion in Groundwater and the Capillary Fringe," *Journal of Contaminant Hydrology* **58**: 111–28.

Lenhard, R. J., and J. C. Parker. 1990. "Estimation of Free Hydrocarbon Volume from Fluid Levels in Monitoring Wells," *Ground Water* **28**: 57–67.

Liu, Z. 2004. *A Study of Bench-Scale Accelerated Weathering Experiments*, Ph.D. Dissertation, Arizona State University, Tempe.

Lundegard, P. D., and P. C. Johnson. 2004. "A Composite Plume Approach for the Analysis of Dissolved Contaminants in Ground Water vs. Distance from Source Areas," *Ground Water Monitoring and Remediation* **24**(3): 69–75.

Lundegard, P. D., and P. C. Johnson. 2006. "Source Zone Natural Attenuation at Petroleum Hydrocarbon Spill Sites: II. Application to a Former Oil Field," *Ground Water Monitoring and Remediation* **26**(4): 93–106.

Martin-Hayden, J. M., and G. A. Robbins. 1997. "Plume Distortion and Apparent Attenuation due to Concentration Averaging in Monitoring Wells," *Ground Water* **35**: 339–46.

McNab, W. W. Jr., and T. N. Narasimhan. 1995. "Reactive Transport of Petroleum Hydrocarbon Constituents in a Shallow Aquifer: Modeling Geochemical Interactions Between Organic and Inorganic Species," *Water Resources Research* **31**: 2027.

Miller, C. T., M. M. Poirier-McNeill, and A. S. Mayer. 1990. "Dissolution of Trapped Nonaqueous Phase Liquids: Mass Transfer Characteristics," *Water Resources Research* **26**: 2783–96.

Millington, R. J., and J. M. Quirk. 1961. "Permeability of Porous Solids," *Transactions of the Faraday Society* **57**: 1200–07.

Molson, J. 2002. *BIONAPL/3D: A 3D Model for Groundwater Flow, Multi-Component NAPL Dissolution and Biodegradation.* Ontario, Canada: University of Waterloo.

Morrison, R., R. Beers, and B. Hartman. 1998. *Petroleum Hydrocarbon Contamination: Legal and Technical Considerations*. Foresthill, Calif.: Argent Communications Group.

NRC (National Research Council). 1994. *Alternatives for Groundwater Cleanup*. Washington, D.C.: National Academies Press.

Ortega-Calvo, J. J. and M. Alexander. 1994. "Roles of Bacterial Attachment and Spontaneous Partitioning in the Biodegradation of Naphthalene Initially Present in Nonaqueous-Phase Liquids," *Applied Environmental Microbiology* **60**: 2643–46.

Ortega-Calvo, J. J., I. Birman, and M. Alexander. 1995. "Effect of Varying the Rate of Partitioning of Phenanthrene in Nonaqueous-Phase Liquids on Biodegradation in Soil Slurries," *Environmental Science and Technology* **29**: 2222–25.

Ostendorf, D. W., and D. H. Kampbell. 1991. "Biodegradation of Hydrocarbon Vapors in the Unsaturated Zone," *Water Resources Research* **27**: 453–62.

Prince, R. C., D. L. Elmendorf, J. R. Lute, C. S. Hsu, C. E. Haith, J. D. Senius, G. J. Dechert, G. S. Douglas, and E. L. Butler. 1994. "17α(H),21β(H)-Hopane as a Conserved Internal Marker for Estimating Biodegradation in Crude Oil," *Environmental Science and Technology* **28**: 142–45.

Prommer H. 2006. *PHT3D: A Multicomponent Transport Model for Saturated Porous Media, User's Manual Version 1.6*.

Rifai, H. S., P. B. Bedient, J. T. Wilson, K. M. Miller, and J. M. Armstrong. 1988. "Biodegradation Modeling at an Aviation Fuel Spill Site," *Journal of Environmental Engineering* **114**: 1007.

Ririe, T., and R. E. Sweeny. 1996. "Fate and Transport of Volatile Hydrocarbons in the Vadose Zone," pp. 529–42 in *Proceedings, 1996 NGWA/API Petroleum Hydrocarbon and Organic Chemicals in Groundwater Conference*, Houston.

Ririe, T., R. Sweeny, and S. Daugherty. 2002. "A Comparison of Hydrocarbon Vapor Attenuation in the Field with Predictions from Vapor Diffusion Models," *Soil and Sediment Contamination* **11**: 529–54.

Rockhold, M. L., R. R. Yarwood, and J. S. Selker. 2004. "Coupled Microbial and Transport Processes in Soils," *Vadose Zone Journal* **3**: 368–83.

Salanitro, J. P. 1993. "The Role of Bioattenuation in the Management of Aromatic Hydrocarbon Plumes in Aquifers," *Groundwater Monitoring and Remediation* **13**(4): 150–61.

Salanitro, J. P., L. A. Diaz, M. P. Williams, and H. L. Wisniewski. 1993. "Simple Method to Estimate Aromatic Hydrocarbon Degrading Units (Microbes) in Soil and Groundwater," presented at the International Symposium on Subsurface Microbiology, Bath, England.

Sanders, P. F., and I. Hers. 2006. "Vapor Intrusion in Homes over Gasoline-Contaminated Ground Water in Stafford, New Jersey," *Ground Water Monitoring and Remediation* **26**: 63–72.

Scow, K. M. 1982. "Rate of Biodegradation," ch. 9 in *Handbook of Chemical Property Estimation Methods. Environmental Behavior of Compounds*, W. T. Lyman, W. F. Reehl, and D. H. Rosenblatt, eds. New York: McGraw-Hill.

Stout, S. A., and P. D. Lundegard. 1998. "Intrinsic Biodegradation of Diesel Fuel in an Interval of Separate Phase Hydrocarbons," *Applied Geochemistry* **13**(7): 851–59.

TPHCWG (Total Petroleum Hydrocarbon Criteria Working Group). 1997. *Selection of Representative TPH Fractions Based on Fate and Transport Considerations*, vol. 3, TPHCWG Series. Amherst, Mass.: Amherst Scientific Publishers.

TPHCWG. 1998. *Composition of Petroleum Mixtures,* vol. 2, TPHCWG Series. Amherst, Mass.: Amherst Scientific Publishers.

Vogel, T. M., C. S. Criddle, and P. L. McCarty. 1987. "Transformations of Halogenated Aliphatic Compounds," *Environmental Science and Technology* **21**: 722.

Wilkes, H., H. Willsch, R. Rabus, F. Aeckersberg, P. Rueter, and F. Widdel. 1995. "Compositional Changes of Crude Oils upon Anaerobic Degradation by Sulfate-Reducing Bacteria," pp. 321–23 in *Organic Geochemistry: Development and Applications to Energy, Climate, Environment and Human History: Selected Papers from the 17th International Meeting on Organic Geochemistry*. San Sebastian, Spain: AIOGA.

Wilson, J. T., F. M. Pfeffer, J. W. Weaver, D. H. Kampbell, R. S. Kerr, T. H. Wiedemeier, J. E. Hansen, and R. N. Miller. 1994. "Intrinsic Bioremediation of JP-4 Jet Fuel, in *Proceedings, Symposium on Intrinsic Bioremediation of Groundwater*, Denver.

Xu, M., and Y. Eckstein. 1995. "Use of Weighted Least-Squares Method in Evaluation of the Relationship between Dispersivity and Field Scale," *Ground Water* **33**: 905–08.

Zemo, D. A. 2006. "Sampling in the Smear Zone: Evaluation of Nondissolved Bias and Associated BTEX, MtBE and TPH Concentrations in Groundwater Samples," *Ground Water Monitoring and Remediation* **26**(3): 125–33.

Appendix A

Example Case Study: Determination of Source Zone Depletion Rates due to Physical and Biological Processes—Former Guadalupe Oil Field

EXAMPLE CASE STUDY: DETERMINATION OF SOURCE ZONE DEPLETION RATES DUE TO PHYSICAL AND BIOLOGICAL PROCESSES— FORMER GUADALUPE OIL FIELD

A.1 BACKGROUND AND SITE SETTING

The former Guadalupe Oil Field (GOF) is a 3000-acre property in San Luis Obispo County on the Pacific coast of central California (Figure A-1). The field was operated from 1950 to 1994. From 1955 to 1990, a petroleum distillate liquid, called "diluent," was used as a thinning agent to lower the viscosity of the crude oil (API gravity = 8–12) in production tubing and pipelines. All oil wells were abandoned by 1994.

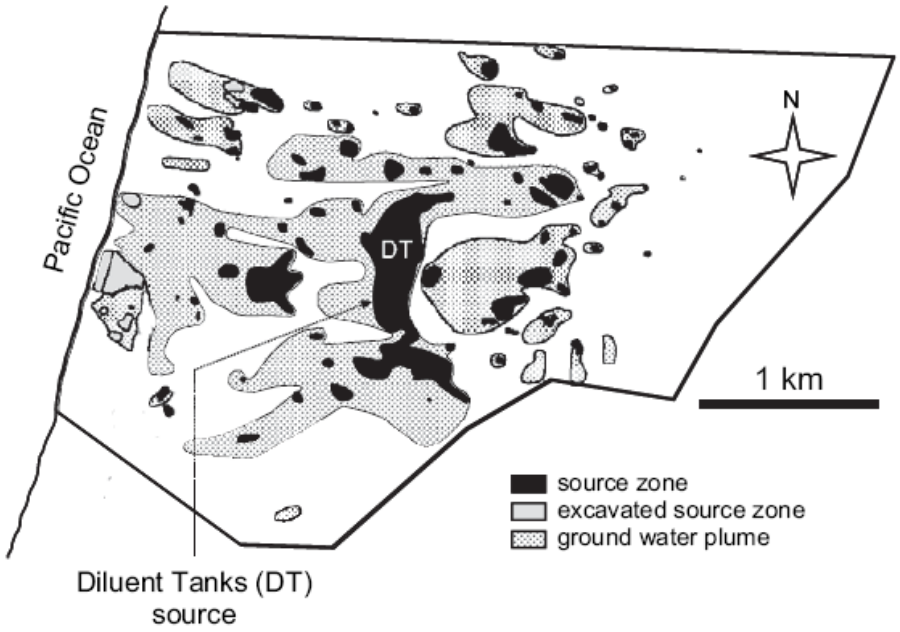

Figure A-1. Map of the former GOF showing source zones and associated dissolved-phase plumes of TPH in groundwater. (*Source*: Lundegard and Johnson 2006).

Inadvertent and undocumented releases of diluent occurred from the distribution system. Many of the releases were of sufficient volume that the diluent percolated down through the surficial dune sands, reached the water table aquifer, and then spread laterally along the water table. Because of the sand dune topography, the depths to groundwater (and hence depths to source zones) vary from very near-surface depths (<1 m) to approximately 45 m (143 feet) bgs. Eighty-three distinct source zones have been identified, with estimated areal extents ranging from approximately 10^2–10^5 m^2 (10^3–10^6 square feet) and containing approximately 10^0–10^5 m^3 of diluent as estimated from diluent saturation profiles. The example NSZD assessment presented in this appendix highlights the diluent tanks (DT) source zone, the largest of source zones (Figure A-1), being approximately 2.3×10^5 m^2 in areal extent and containing approximately 1.2×10^5 m^3 diluent. Additional information is presented in Lundegard and Johnson (2006).

Diluent is an LNAPL. Chemical properties include a boiling point distribution spanning the C_{10} to C_{30} n-alkane range (with a maximum at ~C_{17}), a low content of monoaromatics, polycyclic aromatic hydrocarbons consisting mostly of alkyl naphthalenes, and a high content of polar organic constituents. Due to its high content of polar organic constituents, the water solubility of TPH for diluent samples collected from GOF wells is >1 mg/L, and it varies spatially across the GOF (and even across the larger source zones) from 4 to 30 mg TPH/L·H_2O. The TPH in groundwater at the former GOF consists predominantly of polar organic constituents. The TPH content of affected groundwater is the prime regulatory concern at the GOF. The evaluation of NSZD at this site focused on quantification of TPH mass loss from source zones over time.

A.2 QUALITATIVE ASSESSMENT

Figure A-2 and Table A-1 summarize the representative parameters for the evaluation of NSZD at the DT source zone.

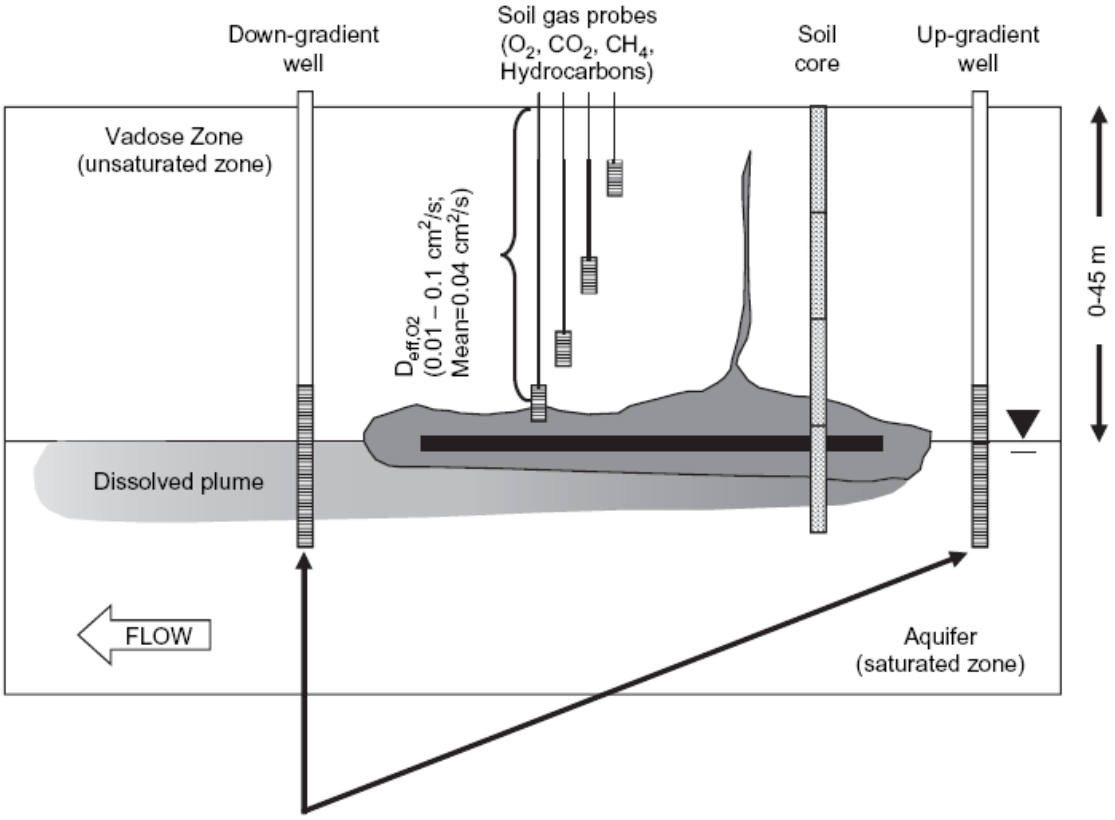

- Dissolved Hydrocarbon Concentrations – (4 – 30 mg/L)
- Electron Acceptor & Transformation Products – (O_2, Fe^{+2}, Mn^{+2}, SO_4^{2-}, NO_3^-, CH_4; AC=3-65 mg-TPH/L)
- Groundwater Table Elevation – (i=0.003-0.005 m/m)
- Hydraulic Conductivity – (K=0.014-0.053 cm/s; geometric mean=0.027 cm/s)

Figure A-2. Schematic cross section showing data used for qualitative and quantitative assessment.

Table A-1. Key qualitative and quantitative parameters used in NSZD evaluation

Item	Value(s)	Comments
Depth to source zone	19 m average	Generally within 1 m of current water table elevation; depth varies because of sand dune topography
Source zone area	2.3×10^5 m^2	Figure A-1
Source zone width perpendicular to groundwater flow	914 m	Figure A-1
Source zone thicknesses	4.6 m	Based on diluent saturation vertical profiles from soil core samples
Source mass estimates	1.2×10^5 kg	Based on diluent saturation profiles and estimated source zone areas
Hydraulic gradient	0.003–0.005 m/m	Flow is primarily east to west (0.004 m/m used in the NSZD calculations)
Hydraulic conductivity	0.014–0.053 cm/s	0.027 cm/s geometric mean used in the calculations
Overall effective vapor phase diffusion coefficient for oxygen	0.038 cm^2/s	Average of vertically averaged values at 11 locations is 0.04 ±0.02 cm^2/s
Diluent solubility in water	7.5–27 mg TPH/L	Based on diluent-water equilibrium tests
Assimilative capacity	5–39 mg TPH/L	Assimilative capacity value described from median values is ~11 mg TPH/L

Biodegradation and dissolution of the submerged part of the source zone was assessed by comparing the chemistry of groundwater upgradient of the source zone with that of groundwater immediately downgradient of the source zone (Table A-2). In brief, the DT source–specific data display the relationships consistent with NSZD: decreased concentrations of dissolved oxygen, nitrate, and sulfate and increased concentrations of dissolved iron and dissolved methane in moving from upgradient to downgradient near-source wells. In addition, the groundwater movement and TPH in groundwater demonstrate that NSZD via dissolution is occurring. Dissolved TPH plumes at the site typically attenuate to <1 mg TPH/L within 1000 feet of the source zone (Lundegard and Johnson 2004).

Table A-2. Summary of dissolved-phase natural attenuation parameter data

	Oxygen (mg/L)	Alkalinity (mg/L $CaCO_3$)	Iron (mg/L)	Nitrate (mg/L)	Sulfate (mg/L)	Methane (mg/L)
Nested wells upgradient of DT source zone						
Data points	5	5	5	5	5	5
Median	2.4	197	0.19	6.1	44	0.003
Minimum	0.8	172	0.06	1.9	23	0.001
Maximum	6.7	245	3.32	40	76	0.014
Nested wells within and downgradient of DT source zone						
Data points	23	26	26	26	26	26
Median	1.2	476	14.7	1.9	9	6.7
Minimum	0.5	280	0.13	1.5	0.7	0.130
Maximum	5.2	608	78	6.5	106	13.3

Soil-gas profiles over sources zones provide evidence of NSZD mechanisms involving vapor phase transport (Figure A-3). All soil-gas profiles show oxygen usage and carbon dioxide production, and, in some cases, methane and hydrogen gas are also observed at the base of the vadose zone. Nonmethane hydrocarbons are present in only very low concentrations because of the semivolatile nature of diluent. The decrease in oxygen, increase in carbon dioxide, and appearance of methane with increasing depth are consistent with the hypothesis that some combination of aerobic and anaerobic biodegradation is occurring in the GOF source zones.

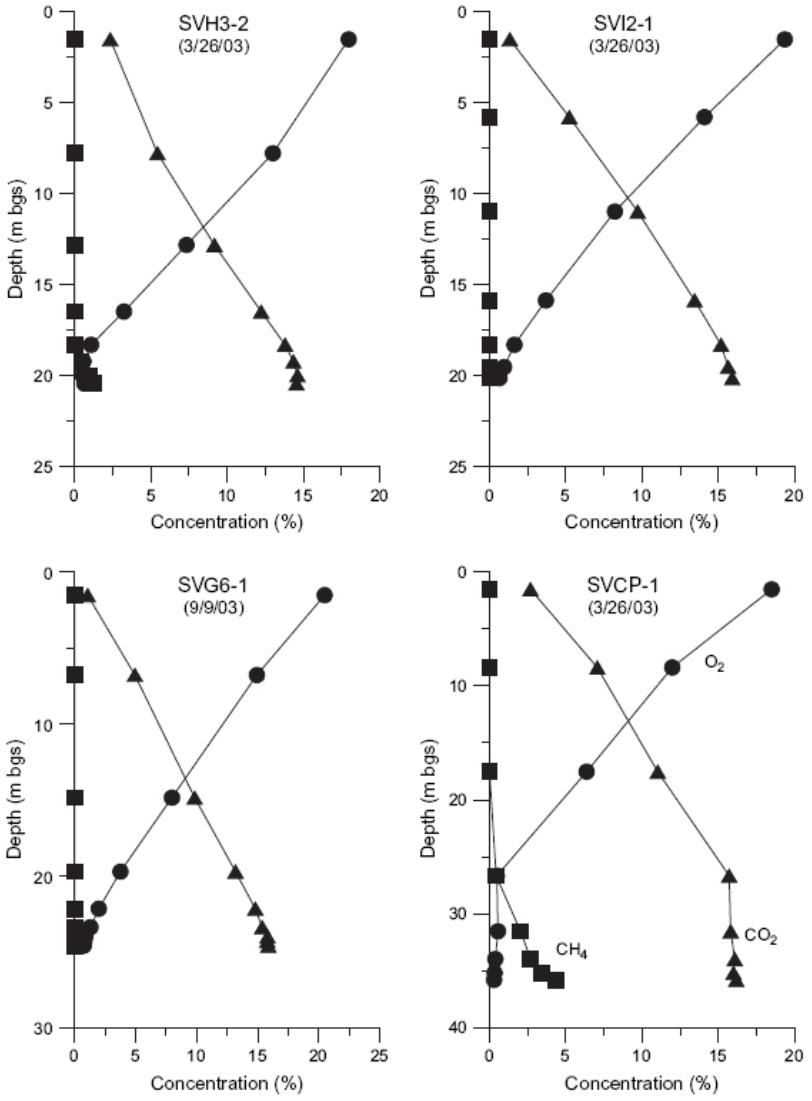

In each example, the deepest data point is ~1 m above the air-LNAPL interface. Little soil contamination exists over the depth range shown.

Figure A-3. Representative soil-gas concentration profiles for oxygen (circles)**, carbon dioxide** (triangles)**, and methane** (squares)**.**

A.3 QUANTITATIVE ASSESSMENT

A.3.1 Estimate of Source Zone Mass Depletion Rate by Dissolution to Groundwater

Flowing groundwater will contact hydrocarbon-affected source zone soils within the saturated zone, and infiltrating precipitation will contact hydrocarbon-affected source zone soils within the vadose zone. In both cases, dissolution of hydrocarbons into the water and a loss of mass from the source occur. A rough estimate of the dissolution rate was made as follows:

$$R_{Dissoln} \approx q_d hw\langle C_d \rangle \qquad \textbf{[Eq. A-1]}$$

where

$R_{Dissoln}$ = estimate of source zone mass depletion rate due to dissolution,
q_d = specific discharge of groundwater through the source zone $\left(\frac{m^3 \cdot H_2O}{m^2 \cdot d}\right)$,
$<C_d>$ = estimate of the area-averaged dissolved concentration at the downgradient edge of the source zone $\left(\frac{kg}{m^3 \cdot H_2O}\right)$,
h = thickness of dissolved-phase constituent plume leaving the downgradient edge of the source zone (m),
w = width of dissolved-phase constituent plume leaving the downgradient edge of the source zone perpendicular to groundwater flow (m).

Dissolution associated with infiltrating rainfall is neglected in Equation A-1 because in the ratio ($I\ L_{source}/q_d\ H_{source}$) << 1 for GOF sources ($I$ = net recharge of precipitation [$m^3\ H_2O/m^2 \cdot d$], L_{source} is the source length parallel to groundwater flow [m]), thereby indicating a negligible dissolution contribution from precipitation relative to groundwater flow through the source (see Section 3.5.2 for additional information). Using the DT source–specific values (Tables A-1 and A-2), a range of possible dissolution rates can be calculated as a function of the source width perpendicular to groundwater flow and source zone dissolved-phase TPH concentration (Figure A-4). For the DT source zone, the estimated range of dissolution mass loss rates is approximately 1100–3900 kg TPH/year.

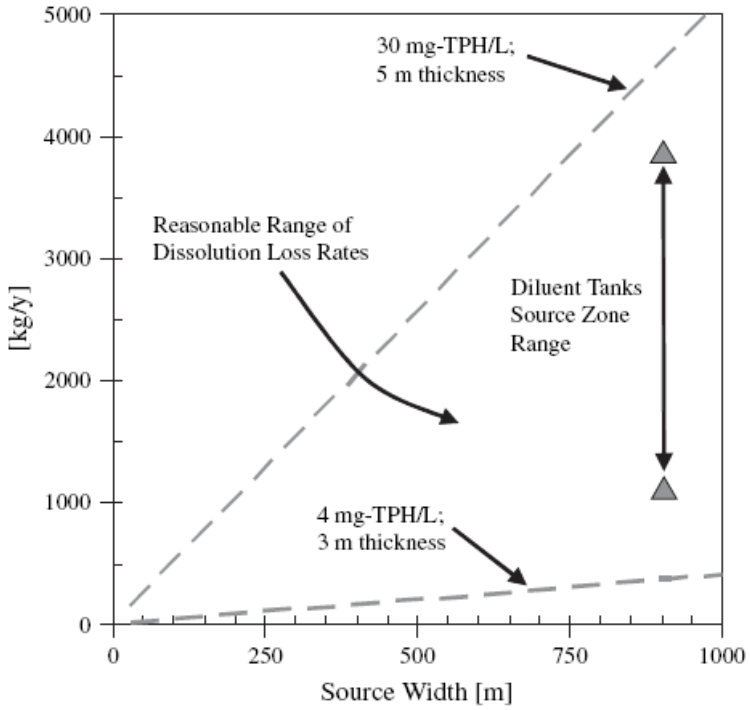

Figure A-4. Dissolution loss rate estimates as a function of source zone width (perpendicular to groundwater flow) and diluent solubility.
Range of reasonable estimates for the DT source zone is shown.

A.3.2 Estimate of Dissolved Source Zone Mass Depletion Rate by Biodegradation

Groundwater flowing into petroleum source zones typically contains electron acceptors that are necessary for aerobic and anaerobic biodegradation reactions (e.g., O_2, NO_3^-, SO_4^{2-}), and groundwater flowing from the source may contain transformation products (e.g., HCO_3^-, CH_4, Fe^{2+}). An estimate of the rate of biodegradation associated with dissolved species transport processes was made as follows:

$$R_{Bio-Sat} \approx q_d HWAC \qquad \textbf{[Eq. A-2]}$$

where

$R_{Bio-Sat}$ = estimate of source zone mass depletion rate due to biodegradation,
AC = the assimilative capacity (mass hydrocarbon/volume H_2O) obtained by taking the difference in the area-averaged dissolved concentrations at the upgradient and downgradient source zone control volume boundaries (kg/m^3 H_2O) for each geochemical indicator (oxygen, nitrate, sulfate, iron-II, manganese-II, methane) multiplied by a representative stoichiometric coefficient for each indicator species (kg-hydrocarbon/kg-species used or produced).

Other terms are defined for Equation A-1.

Electron acceptor delivery associated with infiltrating rainfall is neglected as discussed previously. This macroscopic mass balance approach is nonconstituent specific and therefore can

be used only to estimate the NSZD rate in general (i.e., quantified as TPH degraded with time) via biodegradation.

A range of *AC* values was computed from the maximum and minimum concentrations from all wells upgradient of the source zone (Table A-2) and assuming nondetect downgradient concentrations of electron acceptors and nondetect upgradient concentrations of reaction products (Figure A-5).

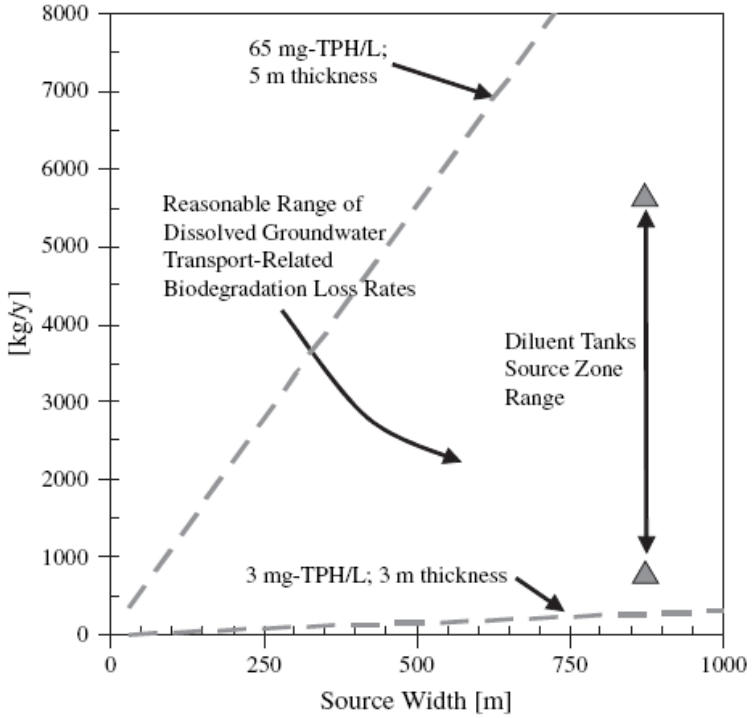

Figure A-5. Mass loss rate estimates as a function of source zone with assimilative capacity.

For the DT source zone, *AC* is estimated to fall in the 5–39 mg TPH/L range, with a median value of 18 mg TPH/L (from data in Table A-2). Of the 18 mg TPH/L, sulfate reduction accounts for 46%, methanogenesis for 41%, denitrification for 6%, aerobic oxidation for 4%, and iron reduction for 3%. Using the mapped width of the DT source zone (915 m), a mass loss rate estimate of 700–5600 kg/year was calculated. This is of the same order of magnitude as the loss rates estimated due to dissolution alone.

A.3.3 Estimate of Source Zone Mass Depletion Rate by Volatilization and Biodegradation in the Unsaturated Zone

Source zones can undergo mass loss by direct vapor-phase transport of volatile constituents upward through the vadose zone. At the GOF, nonmethane volatile hydrocarbon concentrations are very low in soil-gas samples. Consequently, source zone mass loss by direct volatilization is of little significance compared to other processes. Source zones can also undergo mass loss by processes related to the downward diffusion of oxygen through the vadose zone and associated aerobic biodegradation.

Source zone depletion rates were estimated by calculating the oxygen flux at a hypothetical plane placed just above the depth where the methane, oxygen, and any other hydrocarbon concentrations diminish to zero:

$$R_{vapor} \approx WL\left\{S_{O_2} D_{O_2}^T \left(\frac{C_{O_2}^{atm} - C_{O_2}(d)}{d}\right)\right\} \qquad \textbf{[Eq. A-3]}$$

$$\frac{D_{O_2}^T}{d} = \left[\sum_{i=1}^{n} \frac{d_i}{D_{O_2,i}}\right]^{-1}; d = \sum_{i=1}^{n} d_i \qquad \textbf{[Eq. A-4]}$$

where

- D^T_O = the overall effective vapor-phase diffusion coefficient for oxygen vapor between ground surface and a depth d (m^2/time) (see Table A-3),
- $D_{O,i}$ = the effective vapor phase diffusion coefficient for oxygen in layer i (m^2/time) (see Table A-3),
- d_i = the thickness of layer i (m) having effective vapor phase diffusion coefficient $D_{O,i}$,
- C^{atm}_O = the atmospheric oxygen concentration (kg-O_2/m^3-vapor),
- $C_O(d)$ = the oxygen concentration at depth d (usually << C^{atm}_O) (kg-O_2/m^3-vapor).

In this case, S_O ranges approximately 0.25–0.29 kg hydrocarbon/mg O_2 consumed, depending on the relative contributions of direct hydrocarbon aerobic oxidation (0.29 kg hydrocarbon/mg O_2) and indirect hydrocarbon oxidation (0.25 mg hydrocarbon/mg O_2, assuming that methane production occurs first in the anaerobic source zone and then methane is subsequently biodegraded aerobically as it diffuses upward).

Gas transport-related NSZD rates per unit surface area (kg diluent/m^2 surface area/d) were calculated for the vapor sampling locations listed in Table A-3 using a stoichiometric factor (S_O) of 0.29 mg diluent/mg O_2, an oxygen concentration of 300 mg/L vapor (21% v/v) at ground surface, and 0 mg/L vapor (0% v/v) at the depth where diluent contamination, or methane vapor, is encountered.

It was conservatively assumed that the depth at which oxygen is depleted is the same as the depth to groundwater, and the overall effective diffusion coefficients for all six DT source soil-gas clusters were averaged arithmetically. The depth to the source was determined within ArcView; for each square grid, the groundwater elevation was subtracted from the ground surface elevation. The inverse of this value was then areally averaged. Using the DT-specific average effective diffusion coefficient (0.038 cm^2/s), the area-average source depth (18.9 m), and the mapped area of the source zone (231,000 m^2), a source-wide biodegradation rate associated with vapor transport processes of 130,000 kg/year was calculated.

Table A-3. Soil-gas transport-related data and results

Soil-gas probe	Depth (m)	D_{eff}, O_2 (cm^2/s)	Average O_2 concentration (%)	Average D_{eff}, O_2 (cm^2/s)	Biodegradation rate (kg/m^2-yr)
SVH2-1-F	1.5	0.037	17.3		
SVH2-1-E	2.9	0.028	15.3		
SVH2-1-D	5.0	0.026	14.1		
SVH2-1-C	7.5	0.015	4.9		
SVH2-1-B	8.7	0.021	0.6	0.024	7.3×10^{-1}
SVH3-2-H	1.5	0.029	18.3		
SVH3-2-G	7.8	0.028	13.6		
SVH3-2-F	12.8	0.026	7.9		
SVH3-2-E	16.5	0.024	3.7		
SVH3-2-C	19.2	0.026	0.6		3.7×10^{-1}
SVH3-2-A	20.4	0.015	0.8	0.027	
SV12-1-G	1.5	0.049	18.6		
SV12-1-F	5.8	0.044	13.4		
SV12-1-E	11.0	0.077	7.8		
SV12-1-D	15.9	0.050	3.8		
SV12-1-C	18.3	0.031	2.0		
SV12-1-A	20.1	0.020	1.0	0.046	6.0×10^{-1}
SVDT-1-I	1.5	0.041	19.3		
SVDT-1-H	4.6	0.056	16.5		
SVDT-1-G	7.3	0.050	10.1		
SVDT-1-F	9.8	0.085	3.6		
SVDT-1-E	11.0	0.057	1.8		
SVDT-1-C	11.9	0.016	0.6	0.048	1.1
SPTSG-1-H	1.5	0.047	19.2		
SPTSG-1-F	4.6	0.045	17.4		
SPTSG-1-E	7.9	0.049	14.6		
SPTSG-1-D	12.8	0.052	9.4		
SPTSG-1-C	15.3	0.041	5.3		
SPTSG-1-A	17.1	0.042	0.4	0.047	7.3×10^{-1}
SPTSG-2-H	1.5	0.042	19.8		
SPTSG-2-F	4.6	0.036	18.0		
SPTSG-2-E	7.2	0.043	15.6		
SPTSG-2-D	12.0	0.042	10.4		
SPTSG-2-C	14.5	0.047	7.4		
SPTSG-2-A	16.3	0.036	4.3	0.041	6.7×10^{-1}

A.4 CONCLUSIONS

The estimates of source zone mass depletion rates indicate that gas transport processes coupled with biodegradation are responsible for the majority of current source zone mass depletion at the DT source area. Loss rates due to dissolution are roughly comparable to losses controlled by dissolved-phase, transport-related biodegradation in the saturated zone, reflecting the fact that

the assimilative capacity of GOF groundwater is roughly the same magnitude as the solubility of diluent.

Gaining a better understanding of the natural attenuation of petroleum source zones is important to the evaluation of any remedy (including monitored natural attenuation). Documenting NSZD and using field data to estimate the rates of the contributing processes are particularly important. At the former GOF, the qualitative data show that natural attenuation of source zones is occurring throughout the site as a result of several processes, including aerobic and anaerobic biodegradation and dissolution.

Most source zones have exposed and submerged parts, where the exposed part consists of contaminated soil within the capillary fringe or above, and the submerged part consists of contaminated soil below the water table. In general, the quantitative evaluation indicates that NSZD mass loss rates are significantly greater in the exposed parts of the source zones at GOF. The process responsible for the most rapid rate of mass loss is the downward oxygen vapor diffusion that plays a role in direct aerobic biodegradation of petroleum residuals, as well as the oxidation of methane gas generated from anaerobic source zone biodegradation.

Current local rates of mass loss by this process range approximately 0.1–1.0 kg TPH/m^2 area/year. Mass loss by dissolution and biodegradation in the saturated zone are currently approximately two orders of magnitude slower than mass loss associated with oxygen diffusion through the vadose zone. These slower rates will control overall rates of mass loss once aerobically degradable hydrocarbons above the water table are consumed.

A.5 REFERENCES

Lundegard, P. D., and P. C. Johnson. 2004. "A Composite Plume Approach for the Analysis of Dissolved Contaminants in Ground Water vs. Distance from Source Areas," *Ground Water Monitoring and Remediation* **24**(3): 69–75.

Lundegard, P. D., and P. C. Johnson. 2006. "Source Zone Natural Attenuation at Petroleum Hydrocarbon Spill Sites: II. Application to a Former Oil Field," *Ground Water Monitoring and Remediation* **26**(4): 93–106.

CONTACT INFORMATION

Paul C. Johnson, Ph.D.
Arizona State University
Tempe, AZ
(480) 965-9115
paul.c.johnson@asu.edu

Paul D. Lundegard, Ph.D., R.G.
Lundegard USA
Fullerton, CA
(714) 738-5920
paul@lundegardusa.com

Sheila Soderberg
Water Quality Control Board, Central Coast Region
San Luis Obispo, CA
(805) 549-3592
ssoderberg@waterboards.ca.gov

John Catts
Consulting Geochemist
Nicasio, CA
(415) 662-2227
johncatts@earthlink.net

David Peterson, Ph.D.
Stollar - Grand Junction Team/U.S. Department of Energy
Grand Junction, CO
(970) 248-6612
dpeterson57@bresnan.net

Eric Nichols, P.E.
LFR, an ARCADIS Company
Newfields, NH
(603) 773-9779
eric.nichols@lfr.com

Appendix B

Example Case Study: Modeling NSZD Processes—Retail Service Station Release Site

EXAMPLE CASE STUDY: MODELING NSZD PROCESSES— RETAIL SERVICE STATION RELEASE SITE

The following case study is adapted from an energy company's internal NSZD guidance document. This case study focuses on quantifying BTEX NSZD at a former service station site underlain by an aquifer with an LNAPL source.

B.1 BACKGROUND AND SITE SETTING

To calculate NSZD and conversely BTEX persistence, the underlying mechanics of the source area depletion processes were quantified. The calculations were performed using the semianalytic LNAPL partitioning and transport calculation method described in API (2002). This method was selected because it accounts for the primary partitioning and flux mechanisms from LNAPL sources that control NSZD. The method was developed by the American Petroleum Institute (API) to bridge the gap between oversimplistic estimates of partitioning/flux and the complex numerical modeling of multiphase and multiconstituent conditions. The tool accounts for an explicit LNAPL "source" and the multiphase and multiconstituent aspects of the partitioning and transport processes, with certain simplifications to allow the calculations to be performed in an analytic mathematical mode.

Although the following example is based on a simplified service station site, the approach can be applied to larger and/or more complex sites if care is taken to account for parameter variability. Also, although calculations are not presented for this case study, an evaluation of how much a proposed remedial process (air sparging, soil vapor extraction, pump and treat, etc.) conditions will alter NSZD relative to baseline conditions can be conducted using the API LNAPL Dissolution and Transport Screening Tool (LNAST). This type of evaluation can be accomplished by varying input parameters based on remedial measures employed, uncertainty, and sensitivity.

The following example is taken from a former retail service station site where soil and groundwater impacts are present beneath the site. Site investigations have revealed LNAPL and associated dissolved-phase plumes beneath the site. Data collection efforts have demonstrated the stability of the free-product and dissolved-phase plumes. Shallow groundwater is not used in the site vicinity due to elevated total dissolved solids; however, the groundwater may be needed to meet future demand. The future land use for the property will be an unpaved vehicle storage lot on which institutional and engineering controls will be used to eliminate risk pathways to human receptors.

The regulatory authority has a groundwater nondegradation policy that requires cleanup to water quality standards in a reasonable time frame. Consequently, the remaining stakeholder questions for the site revolve around the time frame required to achieve water quality standards, in this case maximum contaminant levels (MCLs). The primary resulting stakeholder question was, "How long will the LNAPL body remain a source of chemical impacts to groundwater at concentrations exceeding MCLs?" The following sections discuss the site data, analysis method, and calculation approach and summarize the calculations and results.

B.1.1 Data Summary

Multiple site investigations have been conducted to assess the LNAPL and dissolved-phase impacts. The following paragraphs summarize data generated during these investigations.

The gasoline release has resulted in an LNAPL body that occupies approximately 10,000 square feet beneath the former underground storage tanks (Figure B-1). Measured LNAPL thickness in wells has historically ranged up to approximately 1 foot in source area monitoring wells but is no longer observed. Groundwater flows from east to west through the source zone with a gradient magnitude of approximately 0.005 ft/ft. Groundwater flow through the source zone has resulted in a stable dissolved-phase plume that extends approximately 175 feet downgradient of the source area. Water table fluctuations have caused the LNAPL body to be smeared across an approximate 4-foot-thick interval throughout most of the source area, as shown in Figure B-1. Cone penetrometer technology and laser-induced fluorescence data were collected along transect A-A′ to gain information on the lithology and source zone thickness. These data are presented later as part of Table B-1 and substantiate a 4-feet smear zone thickness.

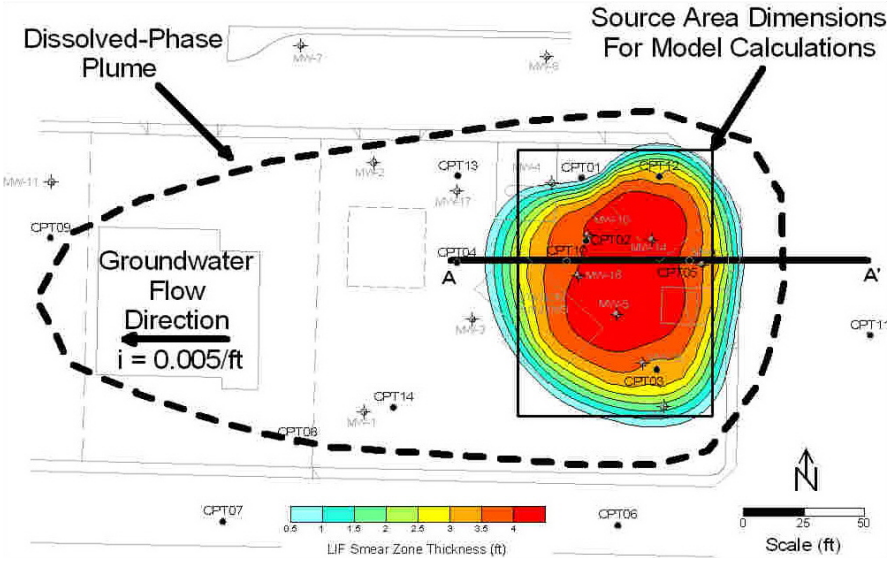

Figure B-1. Areal distribution of LNAPL and dissolved-phase plumes.

The following is a summary of site conditions based on field observations, field testing, and laboratory analysis of soil and fluid samples.

B.1.2 Soil Properties

Saturated Zone Soils. The soils in the saturated zone are fairly homogeneous and consist of poorly graded, fine-grained sands. Slug and pumping tests have been conducted at the site, resulting in an average field-based hydraulic conductivity estimate of approximately 50 feet/day. Porosity ranges from 0.38 to 0.44 and averages 0.41. The van Genuchten capillary properties ("alpha" and "n") were measured in two samples. The "alpha" parameter was 0.4/foot in both samples. The "n" parameter was 2.2 and 2.0. Residual water saturation, both measured and estimated from capillary curves, average approximately 30%.

Vadose Zone Soils. Above the water table, vadose zone soils are interbedded fine-sands and silty-sands to sandy-silts. The finer-grained soils in the vadose zone limit the amount of vapor-phase diffusion from the underlying source zone.

B.1.3 LNAPL Saturation

Soil samples were submitted for chemical analysis of TPH and volatile constituents. TPH results were used to estimate LNAPL saturations. Based on TPH results of samples collected near wells with comparatively thin LNAPL accumulations, the field residual LNAPL saturation is estimated to be approximately 10% in the capillary fringe and water table region. Test results in the vadose zone suggest a lower residual LNAPL saturation of approximately 5% or less. Test results in the core of the source zone suggest peak saturations of approximately 15%. Figure B-2 shows a representative saturation profile developed based on TPH measurements.

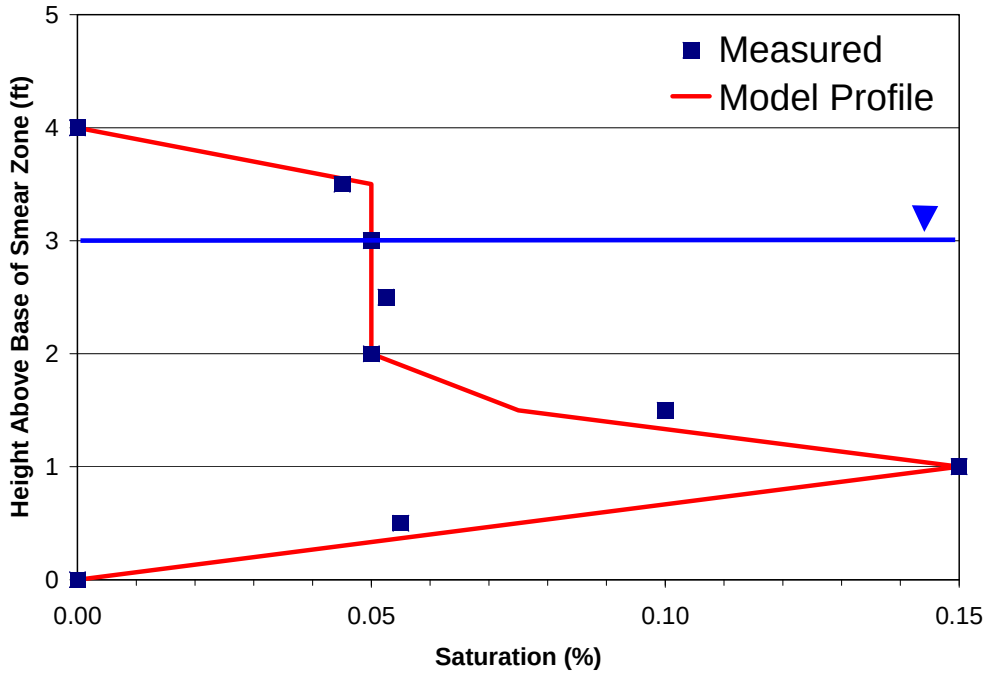

Blue squares show LNAPL saturations estimated from soil TPH chemical analytical results. The red line shows the saturation profile used in the longevity calculations. Note that approximately 75% of the saturation profile is submerged beneath the water table.

Figure B-2. Saturation profile.

B.1.4 LNAPL Properties

The physical properties of the LNAPL were determined from product samples collected from monitoring wells in the source area. The chemical properties of the LNAPL were estimated based on groundwater chemistry using Raoult's Law. The mass fraction of each constituent in the LNAPL was estimated by comparing depth-discrete groundwater sample results collected from the source zone to the pure phase solubility of each respective constituent.

B.2 LNAST MODEL INPUT PARAMETERS

Based on the summary of site conditions presented in Section B.1.1, the input parameters were determined for the constituent flux and NSZD estimates (Table B-1). Most of the parameters listed in Table B-1 are self-explanatory, based on the data summary provided above. Readers who are not familiar with one or more parameters can refer to API (2002) for a detailed review of multiphase physics and multiconstituent partitioning processes. Three parameters—vapor diffusion efficiency, vertical dispersivity, and depth to source zone—require additional explanation.

- **Vapor diffusion efficiency** (VDE) is a model-specific parameter that is used, when necessary, to reduce the calculated vapor flux from the source zone. Any site condition that will limit vapor phase flux leaving the source zone would be reason to use a VDE less than 1. This is the case for our example problem, where the soils overlying the source zone have fine-grained interbeds that limit vapor flux (see Figure B-2). Methods for estimating VDE are beyond the scope of this guidance; interested readers are referred to API (2002) for further detail on this subject.

- A term for **vertical dispersivity** is a required input for the API semianalytic LNAPL partitioning calculation method. Vertical dispersivity is a measure of a dissolved-phase plume's propensity to spread around its center of mass vertically perpendicular to flow. This term is not model specific, and it controls the mass flux of dissolved-phase constituents emanating from the base of the source zone. Constituent transport from the base of the source zone is a complex process involving vertical dispersion and chemical diffusion. In practice, these processes are not easily separated and are typically considered together using a single dispersivity term. This mass flux becomes increasingly important as the length of the source area increases. Vertical dispersivity is difficult to estimate at best and, in many circumstances, can be a very sensitive input parameter. Vertical dispersivity can be estimated by taking 1/100 (Gelhar, Welty, and Rehfeldt 1992) of the longitudinal dispersivity, which in turn is empirically estimated from the length of the dissolved-phase plume (Xu and Eckstein 1995).

- The **depth to the top of the source zone** is a required input for the API semianalytic LNAPL partitioning calculation method when vapor losses are considered. This term is not model specific, and it controls the length of the vapor concentration gradient used in the vapor diffusion calculations. At some sites, where the vapor concentration gradient extends to the land surface, the depth to source zone and concentration gradient length are equal, meaning that there is no biodegradation of vapors in the vadose zone. However, at many sites biodegradation is active, and the vapor profile is truncated at some depth between the source zone and land surface, thus increasing the concentration gradient and vapor flux. At this example site, the vadose zone averages about 25 feet thick. However, soil gas sampling showed that vapor profile was truncated within approximately 10 feet above the source zone. Thus the depth term used in the calculations was 10 feet.

Table B.1. Input parameters for the longevity screening calculations for LNAST

Input parameters	Unit	Value	Rationale
Soil properties			
van Genuchten alpha	(ft^{-1})	0.40	Parameter has narrow range; single average value used.
van Genuchten n	-	2.1	Parameter has narrow range; single average value used.
Saturated hydraulic conductivity (field)	(feet/day)	50	Average value of slug and aquifer tests.
Residual saturation water	%	30	Average of lab tests and values estimated from capillary curves.
LNAPL residual Saturation	%	10	Estimate from TPH analytical results near wells with thin product accumulation.
Porosity	-	0.41	Parameter has narrow range; single average value used.
Vapor diffusion efficiency	-	0.5	Estimated based on equilibrium moisture profiles calculated using measured capillary and petrophysical properties. See text for further explanation.
Groundwater conditions			
Groundwater hydraulic gradient	ft/ft	0.005	Gradient direction is west.
Source area parameters			
Length	feet	80	See Figure B-1.
Width	feet	110	See Figure B-1.
Depth to source zone	feet	10	Length of vapor concentration gradient. See text for further explanation.
LNAPL properties			
Density	g/cc	0.75	Parameter has narrow range, single average value used.
Oil/water interfacial tensions	dynes/cm	20	Parameter has narrow range; single average value used.
Oil/air interfacial tensions	dynes/cm	25	Parameter has narrow range; single average value used.
Viscosity	centipoise	0.6	Parameter has narrow range; single average value used.
Benzene	-	0.01	Estimated from chemical analytical results of depth-discrete source zone groundwater samples using Raoult's law.
Toluene	-	0.06	
Ethylbenzene	-	0.02	
Xylene	-	0.14	
Source area vertical dispersion			
Vertical transverse dispersivity	feet	0.0002 length	Martin-Hayden and Robbins 1997

B.3 SCREENING RESULTS

The following sections summarize the baseline NSZD estimates.

B.3.1 Initial Mass

The calculation tool estimates the initial constituent mass in the source area by considering the source area dimensions, porosity, fluid saturations, and constituent mass fractions. There are a variety of model-specific options for defining the LNAPL saturation. As described above, a

saturation profile based on TPH results was used for screening purposes. With a user-defined saturation profile, the initial mass is then sensitive to only the source area dimensions, porosity, and constituent mass fractions. The mass estimates derived from the model should always be compared with independent mass estimates derived from site data. Figure B-3 shows the initial mass of each constituent present in the LNAPL source zone.

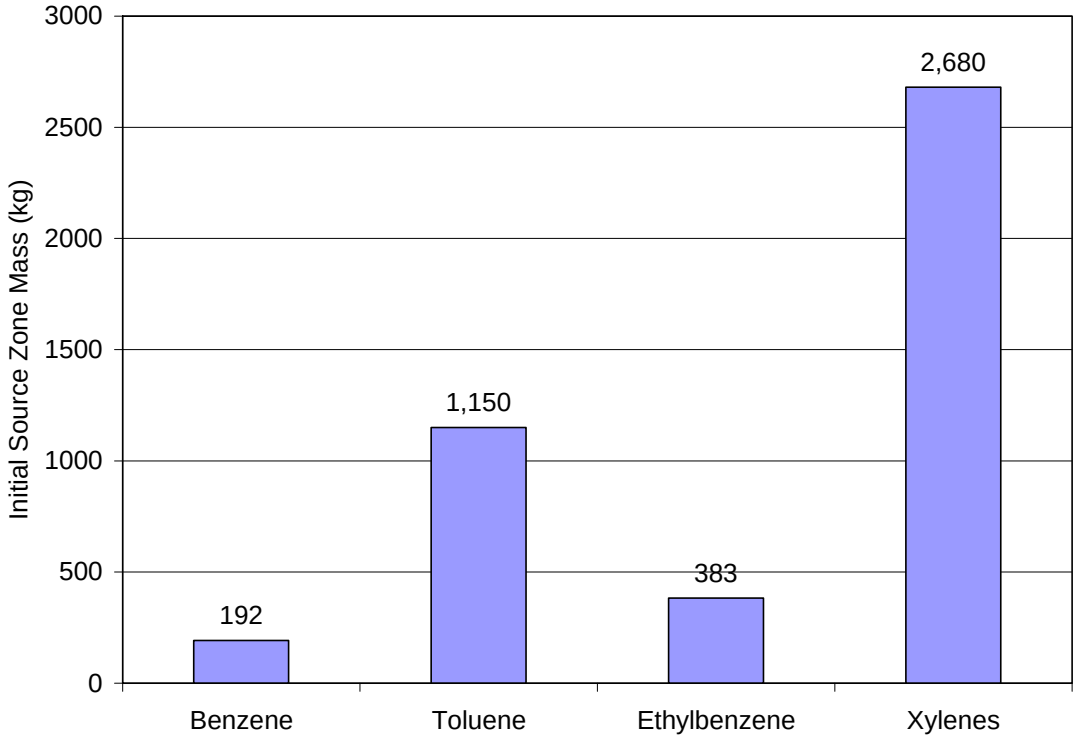

Figure B-3. Initial constituent mass.

B.3.2 Initial Source Area Concentrations and Mass Fluxes

The initial depletion rates in the dissolved- and vapor-phases are a product of the initial source area concentrations and advection and diffusion rates. The dissolved-phase flux is primarily controlled by constituent effective solubility, fluid saturations, capillary properties, hydraulic conductivity, groundwater gradient, and vertical dispersivity. Vapor flux is controlled by constituent effective volatility, capillary properties, vapor diffusion efficiency, and the concentration gradient. Figure B-4 depicts the initial constituent fluxes in the dissolved and vapor phases.

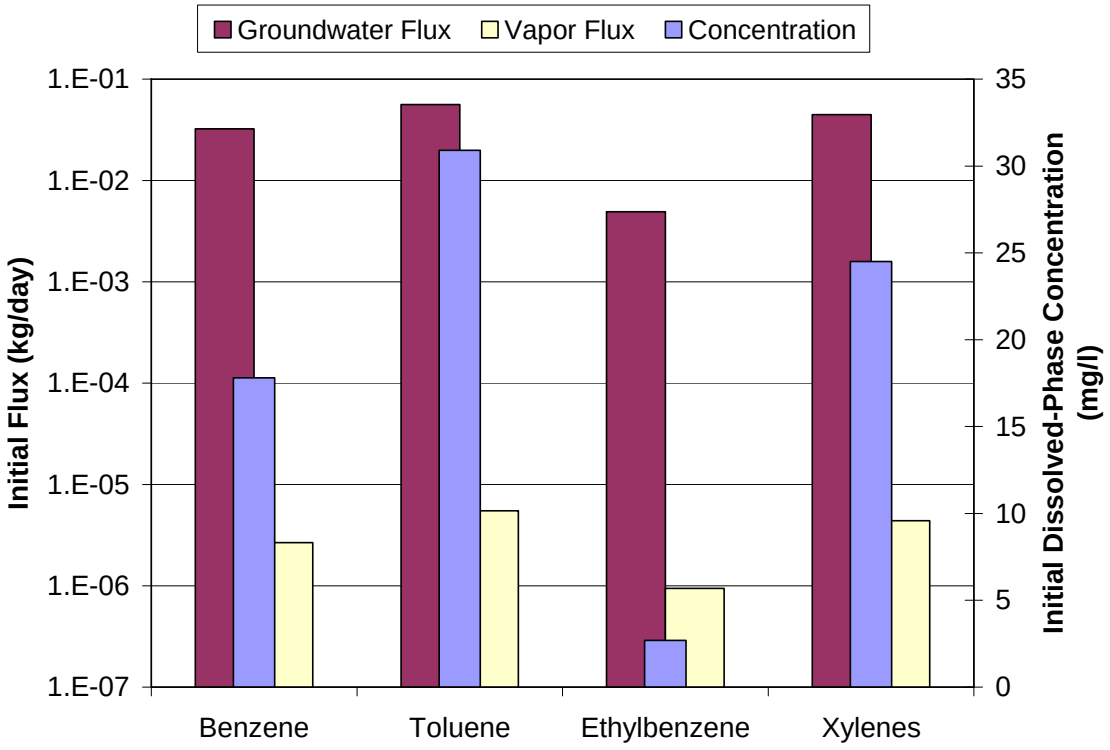

Figure B-4. Initial mass fluxes and source area dissolved-phase concentrations.

The largest groundwater mass fluxes correspond to the largest initial dissolved-phase concentrations and vice versa. Note that the vapor mass flux is many orders of magnitude less than the groundwater mass flux. Comparison of the relative mass flux in dissolved-phase versus vapor-phase illustrates the mass depletion mechanisms operating at the site. The mass loss rate in groundwater is much greater than in the vapor-phase. This outcome might be expected a priori because approximately 75% of the smear zone is submerged.

B.3.3 Baseline NSZD Results

The preceding sections summarized the baseline initial masses and fluxes. The constituent NSZD results are a direct reflection of the constituent mass and fluxes over time. The baseline NSZD (estimated time for source area dissolved-phase concentrations to reach MCLs) is 95, 160, 240, and 140 years for benzene, toluene, ethylbenzene, and xylenes, respectively.

Figure B-5 shows the baseline source area concentrations versus time. Several observations can be made based on review of the figure:

- The constituents with the highest effective solubility, in this case toluene and xylenes, have the largest initial dissolved-phase concentrations and mass flux in groundwater.
- Constituents with the largest initial concentrations and mass fluxes do not necessarily deplete more quickly; the initial mass of the constituent must be considered. In this case, the large initial mass of toluene and xylenes cause these constituents to persist above MCLs longer than benzene, despite their larger mass fluxes.

- Despite its relatively small initial mass, ethylbenzene depletes the slowest due to its low mass flux relative to the other BTEX constituents.
- Benzene depletes most quickly due to its relatively low initial mass and large mass flux.

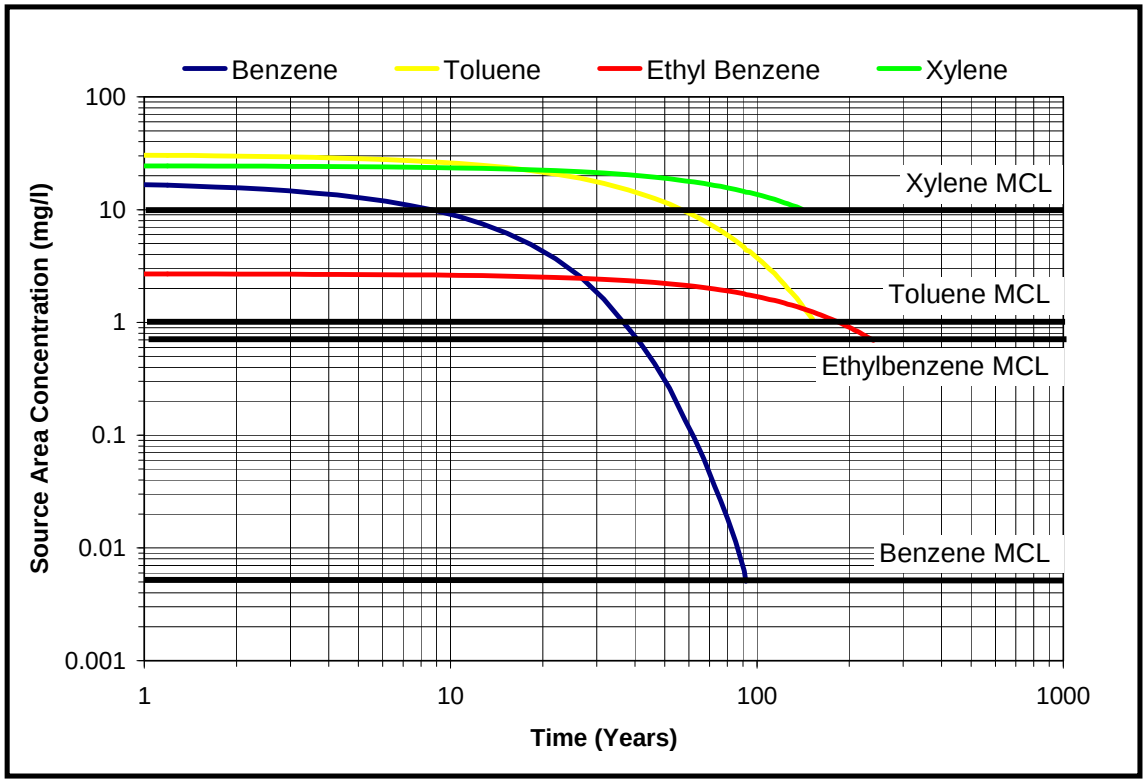

Figure B-5. Baseline longevity results.

Source area concentrations are plotted versus time for each BTEX constituent. Longevity is framed in terms of source area concentration relative to MCLs. Longevity is found by reading the time on the x-axis corresponding to the truncated end of each data series.

B.4 SUMMARY AND CONCLUSIONS

The baseline chemical NSZD for the BTEX constituents is predicted to be 95, 160, 240, and 140 years, respectively. This example had parameter distributions that were fairly homogeneous, and the stakeholder question was not highly detailed. It is important to note that the approaches presented in this case study may not be appropriate for all project sites. Many projects may have heterogeneous parameter distributions or complex source-receptor relationships that will require numerical modeling to answer stakeholder questions. The choice of methods is left to the professional judgment of the project team. In all cases, it is important to compare modeling results to field conditions wherever possible.

B.5 REFERENCES

API (American Petroleum Institute). 2002. *Evaluating Hydrocarbon Removal from Source Zones and Its Effect on Dissolved Plume Longevity and Magnitude.* Publication 4715. Regulatory Analysis and Scientific Affairs Department. Washington, D.C.: API Publishing Services.

Gelhar, L. W., C. Welty, and K. R. Rehfeldt. 1992. "A Critical Review of Data on Field-Scale Dispersion in Aquifers," *Water Resources Research* **28**: 1955–74.

Martin-Hayden, J. M., and G. A. Robbins. 1997. "Plume Distortion and Apparent Attenuation due to Concentration Averaging in Monitoring Wells," *Ground Water* **35**: 339–46.

Xu, M., and Y. Eckstein. 1995. "Use of Weighted Least-Squares Method in Evaluation of the Relationship between Dispersivity and Field Scale," *Ground Water* **33**: 905–08.

Appendix C

Derivation of Some Equations

DERIVATION OF SOME EQUATIONS

C.1 SOURCE ZONE MASS DEPLETION RATE DUE TO DISSOLUTION TO GROUNDWATER

Equation 1—Calculation of Dissolution Rate (R_{diss})

$$R_{diss} = \int_w \int_h Q_d C_d dz dy - \int_w \int_h Q_u C_u dz dy - \int_w \int_h Q_u C_u dz dy - \int_w \int_l Q_r C_r dz dy$$

where

R_{diss}	=	dissolution rate in kg/s,
w	=	width of control volume in m,
h	=	height of control volume in m,
l	=	length of control volume in m,
Q_d, Q_u	=	groundwater discharge at downgradient (d) and upgradient (u) control volume boundaries in m^3-H_2O/m^3-area-s,
Q_r	=	recharge of infiltration water at upper control volume boundary in m^3-H_2O/m^3-area-s,
C_d, C_u	=	dissolved concentration of LNAPL component at downgradient (d) and upgradient (u) control volume boundaries in kg/m^3-H_2O,
C_r	=	dissolved concentration of LNAPL component at upper control volume boundary in kg/m^3-H_2O.

R_{diss} can be approximated as follows:

$$R_{diss} \approx q_d hw \langle C_d \rangle$$

where $\langle C_d \rangle$ = estimate of average dissolved concentration of LNAPL constituent at downgradient control volume boundary in kg/m^3-H_2O.

C.2 SOURCE ZONE MASS DEPLETION RATE DUE TO VOLATILIZATION TO VADOSE ZONE

Equation 2—Calculation of Saturated Zone Biodegradation Rate (R_{biosat})

$$\begin{aligned} R_{biosat} = & \int_w \int_h Q_u \left\{ \left[S_O C_{O,u} \right] + \left[S_N C_{N,u} \right] + \left[S_S C_{S,u} \right] - \left[S_{Fe} C_{Fe,u} \right] - \left[S_{Mn} C_{Mn,u} \right] \right\} dz dy \\ & + \int_w \int_h Q_r \left\{ \left[S_O C_{O,r} \right] + \left[S_N C_{N,r} \right] + \left[S_S C_{S,r} \right] - \left[S_{Fe} C_r \right] - \left[S_{Mn} C_{Mn,r} \right] \right\} dz dy \\ & - \int_w \int_h Q_d \left\{ \left[S_O C_{O,d} \right] + \left[S_N C_{N,d} \right] + \left[S_S C_{S,d} \right] - \left[S_{Fe} C_d \right] - \left[S_{Mn} C_{Mn,d} \right] \right\} dz dy \end{aligned}$$

where

R_{biosat} = dissolution rate in kg/s,
w = width of control volume in m,
h = height of control volume in m,
l = length of control volume in m,
Q_d, Q_u = groundwater discharge at downgradient (d) and upgradient (u) control volume boundaries in m^3-H_2O/m^3-area-s,
Q_r = recharge of infiltration water at upper control volume boundary in m^3-H_2O/m^3-area-s,
C_x,C_u = dissolved concentration of biodegradation component (x) at upgradient (u) control volume boundary in kg/m^3-H_2O,
C_x,C_r = dissolved concentration of biodegradation component (x) at upper control volume boundary in kg/m^3-H_2O,
C_x,C_d = dissolved concentration of biodegradation component (x) at downgradient (d) control volume boundary in kg/m^3-H_2O,
S_x = stoichiometric coefficient for biodegradation process related to biodegradation component (x).

R_{biosat} can be approximated as follows:

$$R_{BioSat} \approx$$

$$WHq_u\left\{\left[S_{O_2}\left\langle C_{O_2,u}\right\rangle\right]+\left[S_{NO_3^-}\left\langle C_{NO_3^-,u}\right\rangle\right]+\left[S_{SO_4^{2-}}\left\langle C_{SO_4^{2-},u}\right\rangle\right]-\left[S_{Fe^{2+}}\left\langle C_{Fe^{2+},u}\right\rangle\right]-\left[S_{Mn^{2+}}\left\langle C_{Mn^{2+},u}\right\rangle\right]-\left[S_{CH_4}\left\langle C_{CH_4,u}\right\rangle\right]\right\}$$

$$+WLq_R\left\{\left[S_{O_2}\left\langle C_{O_2,R}\right\rangle\right]+\left[S_{NO_3^-}\left\langle C_{NO_3^-,R}\right\rangle\right]+\left[S_{SO_4^{2-}}\left\langle C_{SO_4^{2-},R}\right\rangle\right]-\left[S_{Fe^{2+}}\left\langle C_{Fe^{2+},R}\right\rangle\right]-\left[S_{Mn^{2+}}\left\langle C_{Mn^{2+},R}\right\rangle\right]-\left[S_{CH_4}\left\langle C_{CH_4,R}\right\rangle\right]\right\}$$

$$-WHq_d\left\{\left[S_{O_2}\left\langle C_{O_2,d}\right\rangle\right]+\left[S_{NO_3^-}\left\langle C_{NO_3^-,d}\right\rangle\right]+\left[S_{SO_4^{2-}}\left\langle C_{SO_4^{2-},d}\right\rangle\right]-\left[S_{Fe^{2+}}\left\langle C_{Fe^{2+},d}\right\rangle\right]-\left[S_{Mn^{2+}}\left\langle C_{Mn^{2+},d}\right\rangle\right]-\left[S_{CH_4}\left\langle C_{CH_4,d}\right\rangle\right]\right\}$$

where

$<C_x,C_u>$ = estimate of dissolved concentration of biodegradation component (x) at upgradient (u) control volume boundary in kg/m^3-H_2O,
$<C_x,C_r>$ = estimate of dissolved concentration of biodegradation component (x) at upper control volume boundary in kg/m^3-H_2O.
$<C_x,C_d>$ = estimate of dissolved concentration of biodegradation component (x) at downgradient (d) control volume boundary in kg/m^3-H_2O.

C.3 SOURCE ZONE MASS DEPLETION RATE DUE TO VAPOR PHASE BIODEGRADATION IN THE VADOSE ZONE

C.3.1 Equation 3a—Calculation of Volatilization and Unsaturated Zone Biodegradation Rate ($R_{vol\text{-}biounsat}$)

$$R_{vol-biounsat} = \int_w \int_l \left\{ - D_{HC} \left(\partial C_{HC} / \partial z \right) - S_M D_M \left(\partial C_M / \partial z \right) - S_O D_O \left(\partial C_O / \partial z \right) \right\} d_x d_y$$

where

$R_{vol\text{-}biounsat}$ = volatilization and unsaturated zone biodegradation rate in kg/s,
w = width of control volume in m,
l = length of control volume in m,
D_{HC} = effective vapor phase diffusion coefficient for hydrocarbon at depth (d) of horizontal plane in m^2/s,
D_M = effective vapor phase diffusion coefficient for methane at depth (d) of horizontal plane in m^2/s,
D_O = effective vapor phase diffusion coefficient for oxygen at depth (d) of horizontal plane in m^2/s,
$\partial C_{HC}/\partial z$ = vertical concentration gradient of hydrocarbon at depth (d) of horizontal plane in (kg-hydrocarbon/m^3-vapor)/m,
$\partial C_M/\partial z$ = vertical concentration gradient of methane at depth (d) of horizontal plane in (kg-hydrocarbon/m^3-vapor)/m,
$\partial C_O/\partial z$ = vertical concentration gradient of oxygen at depth (d) of horizontal plane in (kg-hydrocarbon/m^3-vapor)/m,
S_M = stoichiometric coefficient for methanogenesis,
S_O = stoichiometric coefficient for aerobic biodegradation.

C.3.2 Equation 3b—Simplified Calculation of Volatilization and Unsaturated Zone Biodegradation Rate ($R_{vol\text{-}biounsat}$)

$$R_{vol-biounsat} = w \left\{ S_O D_{O,avg} \left(C_{O,atm} - C_O / d \right) \right\};$$

$$D_{O,avg} / d = \sum_{i=1} t_i / D_{O,i}$$

$$d = \sum_{i=1} t_i$$

assuming horizontal plane set at depth (d) of 20 m and concentrations of oxygen and methane are negligible at 20 m

where

$R_{vol\text{-}biounsat}$	=	volatilization and unsaturated zone biodegradation rate in kg/s,
w	=	width of control volume in m,
l	=	length of control volume in m,
S_O	=	stoichiometric coefficient for aerobic biodegradation,
$D_{O,Avg}$	=	average effective vapor phase diffusion coefficient for oxygen at from ground surface to depth (d) of horizontal plane in m^2/time,
$C_{O,Atm}$	=	atmospheric oxygen concentration in kg-O_2/m^3-vapor,
C_O	=	oxygen concentration at depth (d) of horizontal plane in kg-O_2/m^3-vapor,
d	=	depth of horizontal plane in m,
t_i	=	thickness of subsurface layer i in m,
$D_{O,i}$	=	effective vapor phase diffusion coefficient for oxygen in subsurface layer i.

Appendix D

Direct Biodegradation of LNAPL

DIRECT BIODEGRADATION OF LNAPL

Biodegradation of LNAPL source zones via microbial activity in the aqueous phase and vapor phase is well documented. However, much less published research is available on the subject of direct intrinsic biodegradation of the nonaqeuous phase in the subsurface. While biodegradation of residual NAPL has been demonstrated (e.g., Stout and Lundegard 1998), it is commonly assumed that biodegradation or mineralization of source zone constituent mass is dominated by the rate of partitioning from the LNAPL to aqueous phase. However, several laboratory studies have shown that rates of mineralization of target constituents dissolved into solvents (NAPLs) have exceeded the measured rates of aqueous-phase partitioning. These studies propose various mechanisms for bacteria to enhance biodegradation of the LNAPL constituents.

D.1 LITERATURE REVIEW

Factors affecting the rate of biodegradation have been investigated by numerous laboratory studies. Birman and Alexander (1996) studied the effect of NAPL viscosity on biodegradation of phenanthrene in several different NAPLs in soil slurries. Efroymson and Alexander (1991, 1994b); Ortega-Calvo and Alexander (1994); and Ortega-Calvo, Birman, and Alexander (1995) found that rates of biodegradation in some cases exceeded the rates of partitioning from NAPL to aqueous phase for reasons discussed below. Inoue and Horikoshi (1991) and Efroymson and Alexander (1994a) describe toxicity effects of organic solvents with low oil/water partition coefficients. Kanaly et. al. (2000) found that a certain microbial growth on diesel fuel likely caused emulsification of the benzo[a]pyrene in diesel fuel.

D.2 MICROBIAL ACTIVITY AND LNAPL

Additional factors also are important to understand biodegradation in LNAPL source zones. The type of the NAPL is important because certain NAPLs may be toxic to microorganisms. Birman and Alexander (1996) found that the extent of mineralization and the mineralization rates of phenanthrene varied depending on into which NAPL the phenanthrene was dissolved (gasoline, kerosene, diesel fuel, fuel oil, or a mixture of the NAPLs). When the target constituent was dissolved in gasoline, a long acclimation phase occurred, indicating that gasoline decreased biodegradation. This study also found that NAPLs of lower viscosity exhibited increased rates and overall extent of biodegradation. NAPLs with low oil/water partition coefficients may be toxic to soil microbes (Inoue and Horikoshi 1991, Efroymson and Alexander 1994a). Additionally, partitioning rates, and, commensurately, bioavailability of dissolved-phase constituents, vary among NAPLs (Ortega-Calvo, Birman, and Alexander 1995; Efroymson and Alexander 1994b).

Importantly, many of the laboratory studies mentioned above selected NAPLs that were not toxic to the microorganisms used for the respective studies. Petroleum releases from contaminated gasoline sites or NAPLs from other sources may have varying degrees of toxicity effects on the available microorganisms. It should also be noted that the microorganism population available to

biodegrade petroleum releases is likely site specific and that, therefore, phenomena observed in laboratory studies may not be observed in the field.

D.3 MICROBIAL EXCRETION OF ENZYMES

Laboratory studies by Efroymson and Alexander (1994b) found that if biodegradation of NAPL constituents is limited by partitioning to aqueous phase, mineralization rates exceeded spontaneous partitioning for a majority of their tests. Further, the bacteria used in this study did not attach themselves to the NAPL. Instead, the study suggests that the bacteria may have excreted enzymes capable of increasing partitioning rates from NAPL to water. This increased partitioning rate served to increase the bioavailability of the target constituent, resulting in an increase in aqueous-phase biodegradation.

D.4 MICROBIAL ATTACHMENT TO THE NONAQUEOUS PHASE

Efroymson and Alexander (1991) note that a bacteria species used in their laboratory study was capable of attaching itself to the solvent-water interface and suggest that the bacteria were capable of degrading the target constituent directly from the nonaqueous phase. Atlas (1981) also notes that hydrocarbon-degrading microbes have been observed growing on the surface of oil droplets, although growth has not been identified *within* an oil droplet without the presence of entrained water. Microbial populations present at the LNAPL-water interface may contribute to the ultimate attenuation of LNAPL at environmental remediation sites.

D.5 BIODEGRADATION OF RESIDUAL LNAPL

Stout and Lundegard (1998) conducted a field study of biodegradation of separate-phase diesel fuel #2 at a diesel fuel production facility. The study concerns residual diesel LNAPL in contact with groundwater collected from a continuous core sample through the separate-phase diesel. Several lines of evidence are presented that would indicate the diesel fuel in the core sample resulted from a single release event. Evidence indicative of intrinsic biodegradation throughout the core sample is suggested by comparison of aliphatic hydrocarbon weight percent and the weight percent of aromatic hydrocarbon, asphaltenes, and nonhydrocarbon constituents across the core; evaluation of both the ratios of pristane to n-C_{17} and phytane to n-C_{18} throughout the core; high-resolution gas chromatogram traces of aliphatic hydrocarbons over the length of the core; and comparison of aliphatic hydrocarbon stable C isotopic compositions across the core. The study found evidence of biodegradation of diesel in the most oil saturated zone (just above the oil-water interface) and below the water table, while areas of the core above the most oil-saturated zone (unsaturated zone) show little or no evidence of biodegradation. See Stout and Lundegard (1998) for a detailed treatment of the study methods and results.

D.6 CURRENT UNDERSTANDING OF LNAPL BIODEGRADATION AND ITS ROLE IN NSZD

The literature documents laboratory and field studies that verified direct biodegradation of LNAPL in certain circumstances. However, EPA (1995) states that, while LNAPL constituents are available for biodegradation in the aqueous phase, it is unlikely that conditions exist within an LNAPL that are favorable for biodegradation. The literature above does not necessarily imply that biodegradation is occurring within the LNAPL itself, but rather implies that bio-activity occurs at the LNAPL-water interface (e.g., enzyme secretion and microbial attachment at LNAPL-water interface). While the laboratory studies confirm that biodegradation of LNAPL does occur in some situations and environments, they also point to circumstances that would reduce or eliminate biodegradation of LNAPL. At many environmental remediation sites, in situ conditions may not be conducive to significant direct biodegradation of LNAPL.

Toxicity of certain LNAPLs (e.g., gasoline) to indigenous microbes may serve to minimize or eliminate direct intrinsic biodegradation as a source mass loss mechanism at some sites. It is also possible that indigenous microbes at some sites may be more or less effective at biodegrading the nonaqueous phase. While intrinsic biodegradation of the nonaqueous phase likely contributes to source zone mass loss at many sites, there are no qualitative or quantitative measurements at present that allow independent measurement of the process. Even though direct biodegradation of the nonaqueous phase is not completely understood at this time, the reader should be aware that biodegradation of the LNAPL body likely occurs at many sites. Additional studies of degradation of residual LNAPL have been published by Douglas et al. 1992 and Prince et al. 1994.

D.7 REFERENCES

Atlas, R. M. 1981. "Microbial Degradation of Petroleum Hydrocarbons: An Environmental Perspective," *Microbiological Reviews* **45**(1): 180–209.

Birman, I., and M. Alexander. 1996. "Effect of Viscosity of Nonaqueous-Phase Liquids (NAPLs) on Biodegradation of NAPL Constituents," *Environmental Toxicology and Chemistry* **15**(10): 1683–86.

Douglas, G. S., K. J. McCarthy, D. T. Dahlen, J. A. Seavy, W. G. Steinhauer, R. C. Prince, and D. L. Elmendorf. 1992. "The Use of Hydrocarbon Analyses for Environmental Assessment and Remediation," pp. 1–21 in *Contaminated Soils: Diesel Fuel Contamination*, P. T. Kostecki and E. J. Calabrese, eds. Chelsea, Mich.: Lewis Publishers.

Efroymson, R. A., and M. Alexander. 1991. "Biodegradation by an *Arthobacter* Species of Hydrocarbons Partitioned into an Organic Solvent," A*pplied Environmental Microbiology* **57**: 1441–47.

Efroymson, R. A., and M. Alexander. 1994a. "Biodegradation in Soil of Hydrophobic Pollutants in Nonaqueous-Phase Liquids (NAPLs)," *Environmental Toxicology and Chemistry* **13**(3): 405–11.

Efroymson, R. A. and M. Alexander. 1994b. “Role of Partitioning in Biodegradation of Phenanthrene Dissolved in Nonaqueous-Phase Liquids, *Environmental Science and Technology* **28**(6): 1172–79.

EPA (Environmental Protection Agency. 1995. *Light Nonaqueous-Phase Liquids*. EPA/540/S-95/500. EPA Groundwater Issue.

Inoue, A., and K. Horikoshi. 1991. “Estimation of Solvent-Tolerance of Bacteria by the Solvent Parameter log P,” *Journal of Fermentation and Bioengineering* **71**(3): 194.

Kanaly, R. A., R. Bartha, K. Watanabe, and S. Harayama. 2000. “Rapid Mineralization of Benzo[a]pyrene by a Microbial Consortium Growing on Diesel Fuel,” *Applied and Environmental Microbiology* **66**(10): 4205–11.

Ortega-Calvo, J. J. and M. Alexander. 1994. “Roles of Bacterial Attachment and Spontaneous Partitioning in the Biodegradation of Naphthalene Initially Present in Nonaqueous-Phase Liquids,” *Applied Environmental Microbiology* **60**: 2643–46.

Ortega-Calvo, J. J., I. Birman, and M. Alexander. 1995. “Effect of Varying the Rate of Partitioning of Phenanthrene in Nonaqueous-Phase Liquids on Biodegradation in Soil Slurries,” *Environmental Science and Technology* **29**: 2222–25.

Prince, R. C., D. L. Elmendorf, J. R. Lute, C. S. Hsu, C. E. Haith, J. D. Senius, G. J. Dechert, G. S. Douglas, and E. L. Butler. 1994. “17α(H),21β(H)-Hopane as a Conserved Internal Marker for Estimating Biodegradation in Crude Oil,” *Environmental Science and Technology* **28**: 142–45.

Stout, S. A., and P. D. Lundegard. 1998. “Intrinsic Biodegradation of Diesel Fuel in an Interval of Separate Phase Hydrocarbons,” *Applied Geochemistry* **13**(7): 851–59.

Appendix E

LNAPL Natural Source Zone Depletion Subteam Contacts

LNAPL NATURAL SOURCE ZONE DEPLETION SUBTEAM CONTACTS

Charles D. Stone, P.G., P.E.
NSZD Subteam Leader
Texas Commission on Environmental Quality
512-239-5825
cstone@tceq.state.tx.us

William "Tripp" Fischer, P.G.
LNAPL Team Leader
Delaware Dept. of Natural Resources and Environmental Control
302-395-2500
william.fischer@state.de.us

Chet Clarke, P.G.
LNAPL Team Program Advisor
AMEC Geomatrix, Inc
512-494-0333
chet.clarke@amec.com

Lily Barkau
Wyoming Dept. of Environmental Quality
307-777-7541
lbarka@state.wy.us

Harley Hopkins
eatmocrawfish@mac.com

John Menatti, P.G.
Utah Dept. of Environmental Quality
801 536-4156
jmenatti@utah.gov

Eric Nichols, P.E.
LFR (ARCADIS)
603-773-9779
eric.nichols@lfr.com

Joel D. Padgett
South Carolina Dept. of Health and Environmental Control
803-896-6398
padgetjp@dhec.sc.gov

Issis Rivadineyra
Naval Facilities Engineering Services
805-982-4847
issis.rivadineyra@navy.mil

Tim J. Smith
Chevron Energy Technology Co.
510-242-9007
tjsmith@chevron.com

John Surber, Jr.
Virginia Dept. of Environmental Quality
276-676-4823
jdsurber@deq.virginia.gov

Lesley Hay Wilson, Ph.D.
Sage Risk Solutions LLC
512-327-0902
lhay_wilson@sagerisk.com

David Zabcik
Shell Oil Products (LSDR)
713-241-5077
david.zabcik@shell.com

Appendix F

Acronyms

ACRONYMS

AC	assimilative capacity
API	American Petroleum Institute
ASTM	ASTM International, formerly American Society for Testing and Materials
BEG	Bureau of Economic Geology
bgs	below ground surface
BTEX	benzene, toluene, ethylbenzene, xylenes
DT	diluent tank
EPA	(U.S.) Environmental Protection Agency
GOF	Guadalupe Oil Field
ITRC	Interstate Technology & Regulatory Council
LNAPL	light, nonaqueous-phase liquid
LNAST	LNAPL Dissolution and Transport Screening Tool
MCL	maximum contaminant level
NAPL	nonaqueous-phase liquid
NRC	National Research Council
NSZD	natural source zone depletion
TPH	total petroleum hydrocarbon
VDE	vapor diffusion efficiency